VOL. 7 No. 2, pp. 33-64 FEBRUARY 1942

Philips Technical Review

DEALING WITH TECHNICAL PROBLEMS
RELATING TO THE PRODUCTS, PROCESSES AND INVESTIGATIONS OF
N.V. PHILIPS' GLOEILAMPENFABRIEKEN
EDITED BY THE RESEARCH LABORATORY OF N.V. PHILIPS' GLOEILAMPENFABRIEKEN, EINDHOVEN, HOLLAND

Dr. G. L. F. PHILIPS †

The founder of our concern, Dr. Ir. G. L. F. Philips, passed away at The Hague on January 26th 1942. Since 1891, the year in which he founded, with his father as sleeping partner, the firm of Philips & Co., till 1922, when he resigned as Managing Director of the N.V. Philips' Gloeilampenfabrieken, he employed his talents as man and engineer for one sole aim, that of making ever better incandescent electric lamps. Thus he built from the ground up and brought to perfection the manufacture of four kinds of lamps, *viz.*, the carbon lamp, the sprayed tungsten wire lamp, the drawn tungsten wire lamp and the gas-filled lamp. In this way he has made the Philips lamp famous in every part of the world. Under his stimulating leadership many ingenious machines for the manufacture of incandescent lamps and parts thereof were designed and made, which even to this day still form the foundation of modern incandescent lamp and radio valve manufacture.

The significance that he attached to science as a powerful aid to the development of the industry manifested itself in 1914 in the establishment of the Philips physical laboratory, where since that time new sources of light, the gas discharge lamps, have been developed and where the cradle has been and still is of many an extension of our company's activities.

THE DEVELOPMENT OF BLENDED-LIGHT LAMPS

by J. FUNKE and P. J. ORANJE.

621.327.9

Blended-light lamps are sources of white light composed of a mercury tube in series with a filament, which can be connected to the A.C. mains without any auxiliary apparatus. In this article several problems are discussed which are connected with the construction of these lamps. Special attention is paid to the measures which must be taken to obtain the desired blending ratio, namely equal amounts of mercury light and incandescent lamp light. In conclusion information is given about a newly developed blended-light lamp of only 300 Dlm, 160 W.

The blending of different kinds of light is at present an important aid in lighting technique. It is particularly important in connection with the employment of high pressure mercury lamps, since their colour rendering requires improvement when they are used because of their high efficiency for general lighting purposes. This improvement in colour was realized chiefly in two ways: the admixture of a certain amount of fluorescence light which is excited by the ultraviolet radiation emitted by the mercury lamp itself, or the admixture of ordinary electric light.

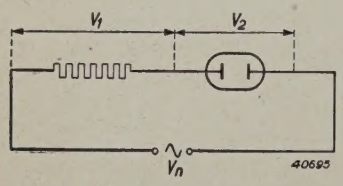

Fig. 1. Diagram showing the principle of the blended light lamp: a filament and a discharge tube in series

In addition to the simple combination of separate mercury and filament lamps in one fitting, a nice solution of the latter problem has recently been devised, which consists in connecting to the mains in series a mercury discharge tube and a filament, housed in the same envelope (see *fig. 1*). The advantages of this system have already been discussed in this periodical [1]): a lamp is obtained with a pleasant colour and with a considerably higher efficiency than the filament lamp, while the auxiliary apparatus necessary with mercury and other metal vapour lamps is eliminated, since the filament itself takes over its function. The lamp may therefore be connected directly to the A.C. mains [2]).

In designing such lamps a number of problems arose which will be discussed in the folowing. We shall first consider the behaviour of a mercury discharge tube burning in series with a resistance.

The variation of the tension on a mercury discharge burning in series with a resistance on an A.C. mains is represented in *fig. 2*. The gas discharge is extinguished twice per period, namely when the mains voltage falls below the value V_b in fig. 2, and it remains extinguished until the mains voltage reaches the re-ignition value v_{rign}. The time interval between extinction and re-ignition of the tube, the "dark period" δ, as may be seen from the figure, is dependent on the size of v_{rign}, and this in turn depends upon the value of the arc tension. At higher arc tensions the time at which the discharge is extinguished is shifted to an earlier moment, which results in an increase in δ. An increase of δ, however, results in a higher re-ignition voltage, because the number of free electrons and ions present falls when no current is flowing, so that a higher voltage is required to initiate the discharge again. For the arc tension we can choose a maximum value such that the re-ignition voltage is equal to the peak value of the mains voltage, since otherwise the discharge no longer re-ignites. For the sake of reliability a considerable margin will be allowed for surges in the mains voltage such as may occur in practice, for example upon switching on large machines.

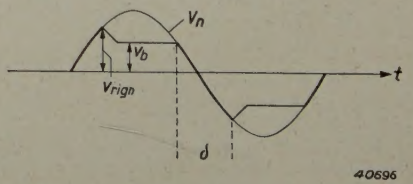

Fig. 2. Variation of the tension on a discharge tube which, in series with a resistance, is connected to a sinusoidal A.C. voltage V_n. At each current alternation the lamp is extinguished, and it is only re-ignited when the mains voltage has reached a certain value v_{rign}, which is higher than the constant value V_b of the arc tension in the remainder of the half period. This causes the occurrence of a dark period (δ).

[1]) Philips Techn. Rev. 5, 341, 1940.

[2]) An advantage of alternating current is that with a given value of the effective voltage the peak voltage is a factor 1.4 higher, so that the discharge tube is easily ignited. On the other hand direct current would have the advantage that the tube would only need to be ignited once, while with alternating current this must be done anew every half period. Blended-light lamps for direct current, however, have not yet appeared on the market.

The difference between the arc tension and the mains voltage must be taken up by the filament. Since the arc tension of the discharge tube is not constant, but begins with a very low value upon switching on the lamp, considerable overloading of the filament may occur when the lamp is switched on. In order to limit also this overloading it is desirable that the arc tension should not be chosen too high.

The whole problem becomes still more complicated because of the fact that we are not only interested in the reliability of the mercury discharge tube and the life of the filament, but we also make certain requirements as regards the efficiency and the colour. In the following therefore we shall go somewhat deeper into the problem of the voltage distribution between filament and mercury discharge in order to demonstrate how a satisfactory compromise was reached between the various requirements.

The voltage distribution

With a discharge tube of given dimensions it is in general possible to choose different values for the arc tension. The arc tension of a mercury discharge is very low at the beginning when the tube is still cold, and the final value is only gradually reached as the mercury pressure increases until all the mercury is evaporated, or, if there is an excess of mercury, until the final stationary state is reached. The larger the series resistance is chosen, the lower the current remains and thus the temperature of the mercury lamp. Its arc tension therefore also remains lower. In this way a very wide range of arc tensions can be realized practically.

The arc tension is made up of a steep voltage drop at cathode and anode (cathode drop and anode drop) and a gradual voltage drop along the tube. This gradual voltage drop increases very much as the mercury pressure increases, while on the contrary cathode drop and anode drop decrease slightly in that case.

Since the energy dissipated in the cathode and anode drops furnishes practically no contribution to the luminous flux, it is immediately clear that the efficiency of the mercury lamp increases with increasing arc tension. Actually the improvement is even more significant than would be concluded from this, since the efficiency of the light excitation itself is also found to increase with increasing voltage drop per cm length of the column [3]). In *fig. 3* an example is given of the combined action of the two effects. If, finally, one does not consider the mercury discharge alone, but the combination of discharge tube and filament in series, a relatively still greater improvement of the efficiency is observed. With increasing arc tension the ratio of mercury light to filament light is shifted in favour of the mercury light, and this is advantageous for the overall efficiency, since the mercury lamp possesses a considerably higher efficiency than the filament lamp. We may thus conclude that it is extremely important, as far as the efficiency is concerned, to have the discharge tube take up as large a part of the mains voltage as possible.

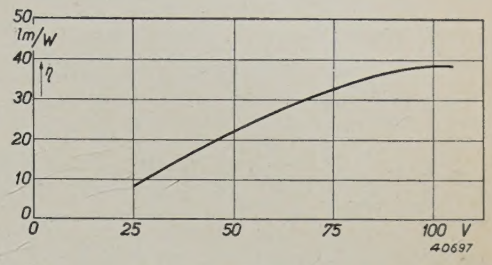

Fig. 3. Increase of the efficiency η of a high pressure mercury discharge with increasing arc tension.

In order to obtain a better and more numerical idea of the conclusions reached in the foregoing, let us consider the energy consumed by discharge tube and filament. The currents are the same for both at every moment, so that the division of the energy dissipation at each moment is given by the division of the voltage. If we pass from momentary values to effective values we may write the following for the energy of the filament:

$$W_1 = I \; V_1,$$

while the energy of the discharge tube must be expressed in the form

$$W_2 = a \; I \; V_2.$$

The factor a, which may have a value of 0.7 for example, expresses the fact that the energy consumed by a mercury discharge is smaller than the product of the effective values of current and voltage. Superficially this is the same phenomenon which occurs with chokes and condensers where the phase difference between current and voltage is the cause; a is then equal to the cosine of the phase angle.

In the case also of the mercury lamp one speaks of a kind of phase shift, since the current in each direction only begins to flow when the voltage in that direction has reached a certain minimum value (the re-ignition value). This apparent phase shift, however, has no well defined significance, since the variation of current and voltage deviates very much from the sine form, which of itself also results in a decrease

[3]) A theoretical consideration of the efficiency of the mercury vapour discharge may be found in Philips Techn. Rev. **1**, 2, 1936.

of a. Therefore we shall designate a by the name of power factor.

If the power factor of the mercury tube is known and also the efficiencies η_1 and η_2 of filament and mercury discharge, the overall efficiency η of the lamp and the blending ratio M (luminous flux of mercury discharge divided by luminous flux of filament) can be given as a function of the voltage division. It is found that

$$\eta = \frac{V_1\eta_1 + a\,V_2\eta_2}{V_1 + a\,V_2} \quad \ldots\ldots \text{(1a)}$$

$$M = a\,\frac{V_2\eta_2}{V_1\eta_1} \quad \ldots\ldots\ldots \text{(1b)}$$

From this it follows that the blending ratio increases not only with the arc tension V_2 but also with the factor a. Since $\eta_2 < \eta_1$, this means at the same time an increase of the total efficiency η. In order to obtain as high an efficiency as possible, it is therefore desirable to make not only the arc tension but also the power factor as large as possible.

The influence of the power factor on the efficiency and the blending ratio is actually less simple than would be concluded from equation (1). When the arc tension V_2 has been chosen, the voltage drop V_1 on the series arc tension at a given mains voltage V_n is not yet determined but depends upon the power factor. For sinusoidal voltages with equal phase ($a = 1$) the following is naturally valid:

$$V_1 + V_2 = V_n, \ldots\ldots\ldots \text{(2)}$$

i.e. the sum of the effective voltage on series resistance and mercury discharge is equal to the effective mains voltage. If, however, there is a phase difference ψ ($\cos\psi = a$) between the voltages on series resistance and mercury discharge, then

$$V_n^2 = V_1^2 + V_2^2 + 2\,V_1V_2\,a, \ldots\ldots \text{(3)}$$

from which it may easily be deduced that the sum of the effective voltages V_1 and V_2 begins to be greater than the mains voltage. If the value of a is not determined by a phase shift, but by the distortion of current and voltage, as is the case when a filament is employed as series resistance, equation (3) is also found to be valid.

The relation between V_n, V_1, V_2 and a results in the fact that at constant mains voltage and arc tension the power supplied to the mercury discharge not only becomes greater with increasing power factor but at the same time the power supplied to the filament decreases (V_1 becomes smaller). The influence of the power factor on efficiency and blending ratio is thus thereby reinforced.

Considerations from the point of view of lighting engineering and conclusions

Until now in discussing the voltage and power factor we have considered only the economic factors. The question of the blending ratio of mercury light and filament light was also only considered in connection with its effect on the overall efficiency. If now on the basis of the factors discussed we reach a certain compromise, we must still consider whether the result satisfies our requirements from the standpoint of lighting engineering. The mixing of mercury light and filament light was indeed done in order to improve the colour.

On the basis of experience with numerous installations in which filament lamps and mercury lamps are installed side by side, a blending ratio of equal amounts of mercury and filament light may be recommended for general applications. By far the majority of all blended-light installations are designed on this basis. It is thus obvious that in the case of the blended-light lamp the goal should be a blending ratio $M = 1$.

As we have seen from equation (1b), the blending ratio is determined mainly by the arc tension V_2 and the power factor a. The question thus arises whether the desired blending ratio can be realized with an arc tension which is high enough to give a reasonable efficiency but not so high that difficulties may occur in re-ignition. It is now found that in practice the latter requirement is difficult to satisfy: if for example a discharge tube with a power factor $a = 0.7$ is chosen, a blending ratio of only about $M = 0.85$ can be obtained. A further increase of M is only possible by improving the power factor, and it was along this line in fact that the desired goal was attained.

In order to improve the power factor a it was important to investigate the factors upon which a depends. In general it may be said that those factors which facilitate the re-ignition will also improve the power factor. The phase shift between current and voltage becomes smaller, the shorter the dark period lasts.

In agreement with anticipation it was found that with increasing distance between the elec-

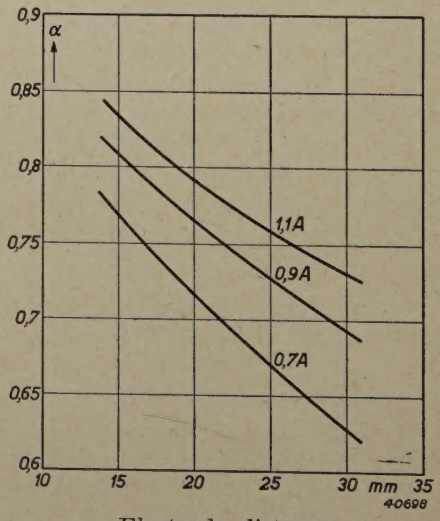

Fig. 4. Power factor a of a mercury discharge tube as a function of the distance between the electrodes at different values of the current, measured on a series of tubes with the same arc tension and diameter.

trodes the power factor improves, as may be seen from the measurements reproduced in *fig. 4*. Furthermore in *fig. 5* the experimentally found relation between the power factor and the diameter of the discharge tube is given. This relation has a less simple character. Different factors probably act in opposition to each other here, as may be concluded from the fact that for a certain diameter an optimum is reached. Since this diameter is fairly large we reach the conclusion that it is desirable to make the discharge tube relatively short and wide. By using this method a blending ratio of 1 : 1 was indeed attained.

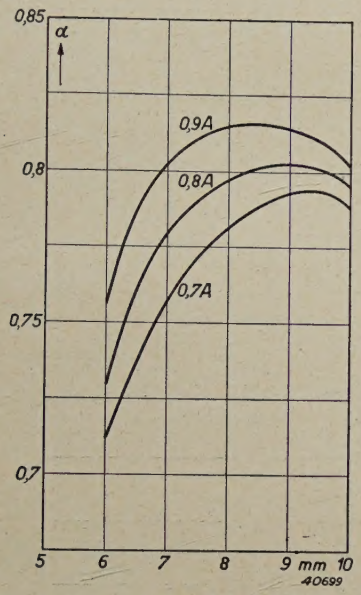

Fig. 5. Power factor a of a mercury discharge tube as a function of the tube diameter at different values of the current, measured on a series of tubes with the same arc tension and distance between the electrodes.

Construction of the blended-light lamp

In addition to the factors already discussed: arc tension, efficiency and blending ratio, in the practical construction of the lamp the power consumed is also important, In general it may be said that mercury lamps of high power can be more easily made than low power units. This peculiarity is illustrated in the fact that mercury lamps for street lighting could be realized much earlier than mercury lamps for interior lighting. In blended-light lamps it is even more difficult to obtain sufficiently small units, since an equal quantity of filament light is added to the mercury light.

The first type brought on the market, which was described in the article cited in footnote [1]), had a power consumption of 250 W and a luminous flux of 500 Dlm. In the meantime a considerably smaller lamp with practically the same efficiency has been successfully developed,

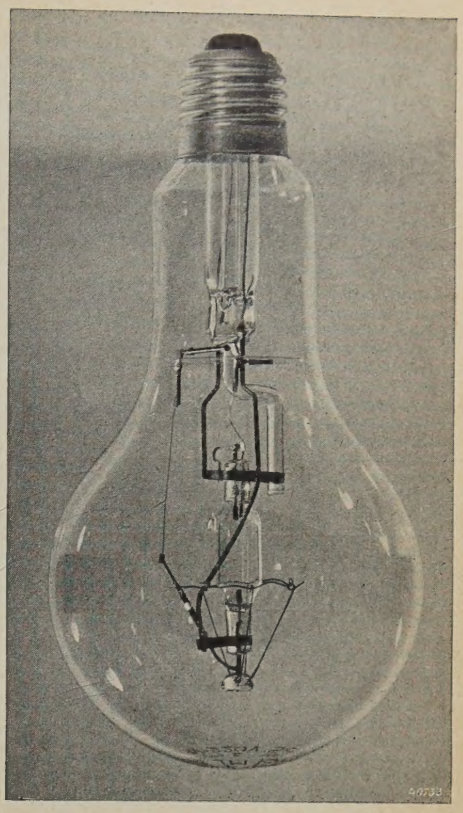

Fig. 6. The blended-light lamp ML 3000. The filament is in the form of a horizontal ring at the height of the arrow.

namely one with a power consumption of 160 W and a luminous flux of 300 Dlm. In *table I* the data of the two lamps are given side by side, while in *fig. 6* the construction of the blended-light lamp ML 300 may be seen.

Table I

Data of the blended-light lamps ML 300 and ML 500

	Unit	ML 300			ML 500		
		Discharge	Filament	Total	Discharge	Filament	Total
Luminous flux	Dlm	150	150	300	250	250	500
Wattage	W	45	115	160	70	180	250
Current	A	0.73	0.73	0.73	1.14	1.14	1.14
Tension	V	78	158	225	78	158	225
Power factor	—	0.79	1.0	0.98	0.79	1.0	0.98

Other properties of the blended-light lamps

As may be seen from the table, the blended-light lamps are designed for a voltage of 225 V. This has been done because of the fact that the effective voltage of so-called 220 V mains usually lies between 220 and 230 V with 225 V as the most frequently occurring value. Filament lamps also are designed for 225 V for various countries where 220/230 V is given as nominal value [4]). In the case of the blended-light lamp, which may be overloaded even less

than a filament lamp [5]), it is of still greater importance that the voltage for which the lamp is designed should be chosen to correspond to the actual voltage of the 220 V mains.

In the interval from 220 to 230 V the blended-light lamps may be used without hesitation. At higher voltages the life of the lamp rapidly decreases, while at lower voltages the efficiency decreases appreciably. If the lamp is burned on a mains voltage which differs from 225 V, current, luminous flux, power consumed and efficiency vary in the manner indicated in *fig. 7*.

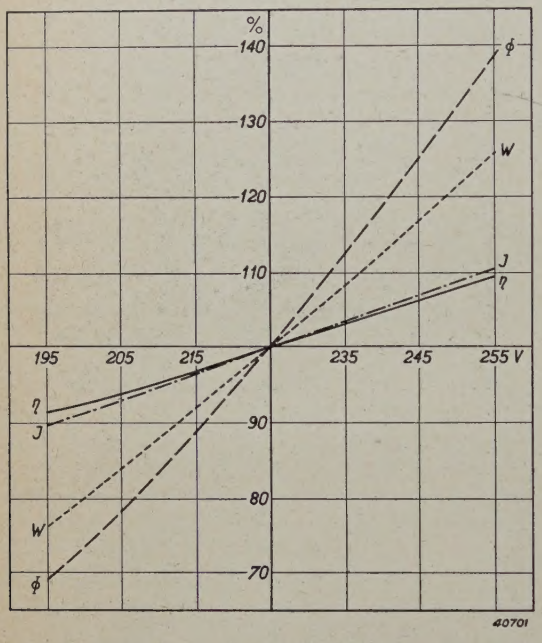

Fig. 7. Variation in current I, luminous flux O, power consumed W and efficiency η upon variations of the mains voltage for the blended-light lamp ML 300.

Under certain circumstances at mains voltages below 200 V, especially in the case of older lamps, difficulties with re-ignition may occur. If (due for instance to the switching on of a heavy load) a temporary large voltage drop occurs on the mains to which blended-light lamps are connected, it is possible that the lamps will be extinguished. The margin allowed for this drop in voltage, however, is large and amounts to about 50 V.

Upon switching on the lamp the applied voltage must be taken up almost entirely by the filament. As the mercury in the discharge tube evaporates the voltage on the filament decreases and the luminous flux from the discharge tube becomes greater, so that the blending ratio, beginning with practically zero, increases as the tube warms up in the manner indicated in *fig. 8*. In *fig. 9* the variation of current, wattage and luminous flux during the heating-up period are plotted.

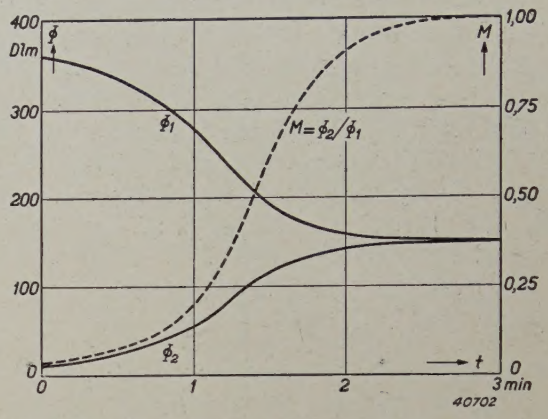

Fig. 8. Variation of the luminous flux Φ_1, resp. Φ_2 of the filament and the discharge tube, and the variation of the blending ratio $M = \Phi_1/\Phi_2$ for the blended-light lamp ML 300 during the heating-up period.

The heavy overloading of the filament each time the lamp is switched on has a strong effect on the life, so that the latter depends upon the time during which the lamp burns between

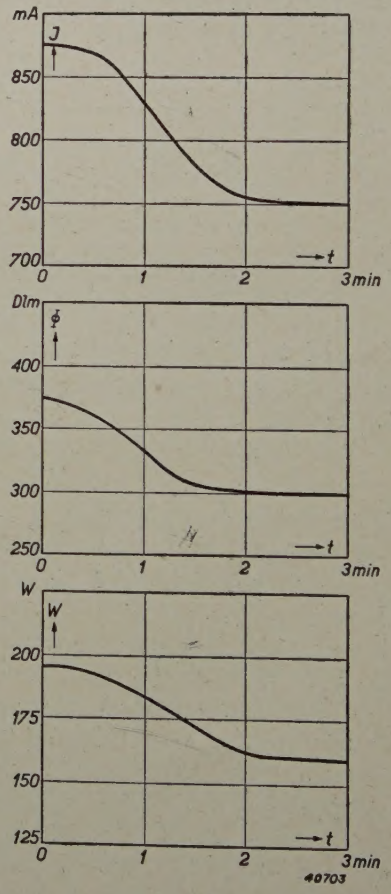

Fig. 9. Variation of the current I, the luminous flux Φ and the power consumed W during the heating-up period for the blended-light lamp ML 300.

[4]) See Philips Techn. Rev. **6**, 334, 1941.

[5]) Upon slight fluctuations of the mains voltage the arc voltage of the mercury tube remains practically constant, so that the whole voltage variation must be taken up by the filament. The voltage variation on the filament is thus increased to a relatively higher degree.

two switching operations. In designing the lamp the calculations were made on the basis of an average life of 2000 hours with 700 switching operations. The overloading of the filament has the advantage that directly after being switched on the lamp gives a satisfactory light output; the luminous flux is even greater than that provided during normal use.

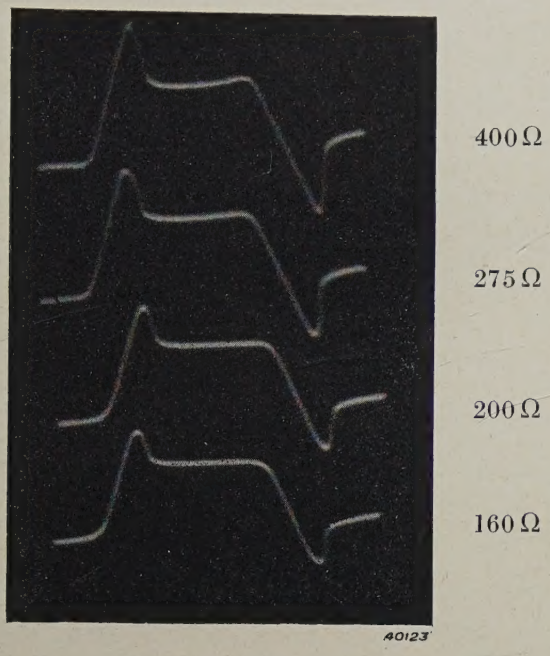

Fig. 10. Oscillograms of the variation of the voltage on a mercury discharge tube which is connected to a constant mains voltage *via* different resistances. It may be seen that the reignition voltage increases with increasing resistance (decreasing current) and that the dark period therefore also becomes longer.

As already noted, the light from the discharge tube is extinguished for a short time (dark period) at each alternation of the current direction. The length of this dark period is determined, among other factors, by the value of the resistance in series. This relation is illustrated by the oscillograms given in *fig. 10*. With increasing resistance the dark period as well as the re-ignition voltage increases.

The occurrence of the dark period gives a strong ripple in the current, which is also manifested in the variation of the light intensity of the mercury discharge. The temperature of the filament follows the fluctuations of the power applied with a retardation (due to its heat capacity) such that the light intensity fluctuates only slightly. The blended-light therefore has a ripple which is considerably smaller than that of the light of a mercury lamp alone. In *fig. 11* oscillograms are given of the light of the discharge tube, the filament and the blended-light lamp.

Due to the fact that the discharge tube is normally used in a vertical position, the greatest

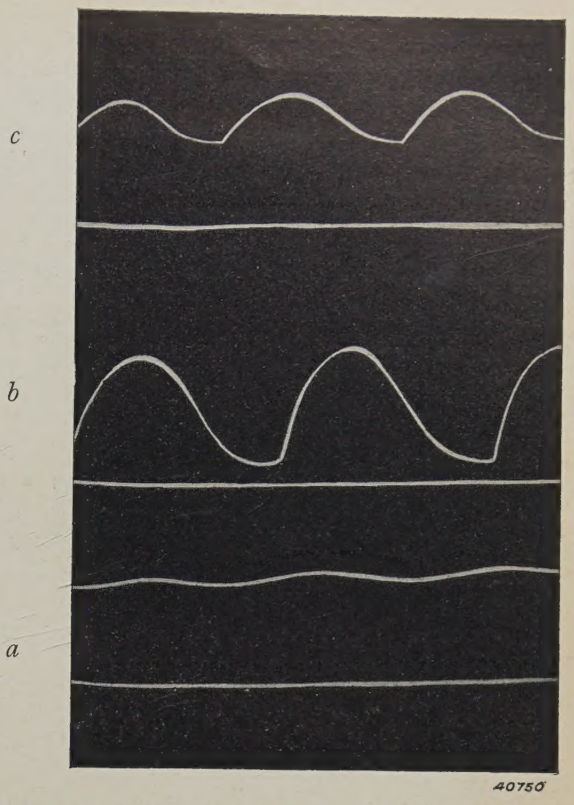

Fig. 11. Oscillograms of the light of the blended-light lamp. *a*) Light from the filament; *b*) light from the mercury discharge; *c*) blended light vertically beneath the lamp. The light from the filament exhibits a smaller ripple than that of the mercury discharge.

light intensity is produced in a horizontal direction, while the filament in the form of a horizontal ring possesses the maximum intensity

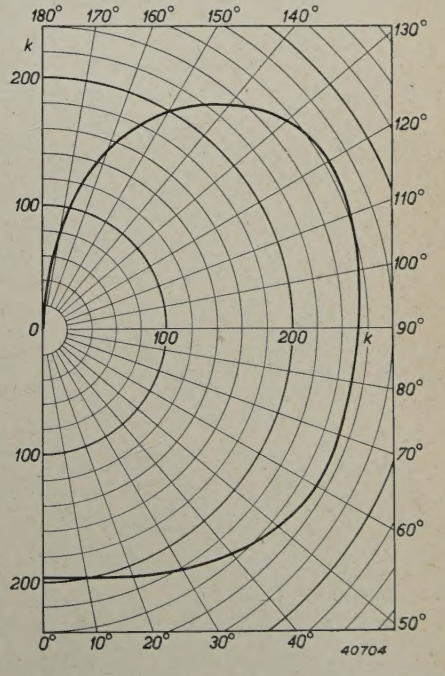

Fig. 12. Candle power distribution of the blended-light lamp ML 300.

in the vertical direction. The candle power distribution of the combination is given in *fig. 12* for a frosted-bulb blended-light lamp, type ML 300.

The possibilities of application of the blended-light lamp were briefly discussed in the article referred to in footnote [1]). Examples given were the lighting of factories, schools, offices, shops and other interiors where large lamp units are desired for illumination. With the new type ML 300 developed since then the possibility of application is appreciably extended in the direction of those cases where smaller lamp units are customarily used.

THE FUNCTIONING OF TRIODE OSCILLATORS WITH GRID CONDENSER AND GRID RESISTANCE

by J. van SLOOTEN. 621.396.615.1:621.396.621.5

In this article an analysis is given of the action of a triode oscillator which is provided in the usual way with a grid condenser and leakage resistance (grid resistance). In particular a study is made of the way in which the A.C. voltage produced and the average anode and grid current vary upon continuous change in the value of the leakage resistance. It is found that the final working state of the oscillator upon excitation of the grid D.C. voltage by means of the circuit elements mentioned may be quite different from that when the same grid D.C. voltage is excited by means of a battery. At the same time the cause of "blocking" is logically revealed.

In the majority of radio receiving sets now in use and in practically all of those now on the market, the superheterodyne principle is applied. The modulation of the high-frequency oscillations of the transmitter received is converted into a constant intermediate frequency by means of a local oscillator, whose frequency is changed from station to station [1]). The very frequent use of small oscillators resulting from this has naturally led to a careful study of their properties and of the special phenomena which are encountered in their use.

A phenomenon which is familiar to all builders of receiving sets is the so-called "blocking" of the oscillator, which has already been discussed in this periodical [2]). As was there shown, the blocking consists of a periodic interruption of the oscillation produced. By itself this phenomenon was already familiar before superheterodyne receivers were built, but for years no really satisfactory information was available as to the circumstances under which it occurs and its actual cause.

This may be explained from the fact that the actual cause has a rather complicated nature and only becomes clear upon a careful consideration of "normal" oscillation. In this article we shall consider this normal oscillation. For reasons which will later become apparent, we shall set about it in two steps, by first considering an oscillator with a control-grid bias which can be permanently set and then discussing the case where the control-grid bias is obtained in the usual way with grid condenser and leakage resistance.

An oscillator with grid bias which can be set

As point of departure we have chosen the connections given in *fig. 1*. In the diagram may be seen a triode, an oscillation circuit consisting of a condenser C and a self-induction L, with which a resistance r must be imagined to be in series, and finally a back-coupling coil in the anode circuit (M here denotes the coefficient of mutual induction with respect to L). The grid voltage V_g is taken from a potentiometer and is measured by the measuring instrument indicated. Further, we assume that the following quantities are measured: the average grid current $\bar{i}_g$, the average anode current $\bar{i}_a$ and the peak value W of the A.C. voltage which occurs on the oscillation circuit as a result of the oscillation.

When we vary the grid voltage by moving the potentiometer, $\bar{i}_a$, $\bar{i}_g$ and W will also change in a definite way. Their dependence is given in *fig. 2*a as measured in a special case. In this figure the static triode characteristic: i_{a_0} as a function of V_g (in the non-oscillating state), is

[1]) On the subject of the superheterodyne principle see Philips Techn. Rev. **1**, 76, 1936.

[2]) Philips Techn. Rev. **3**, 248, 1938 and **5**. 315, 1940.

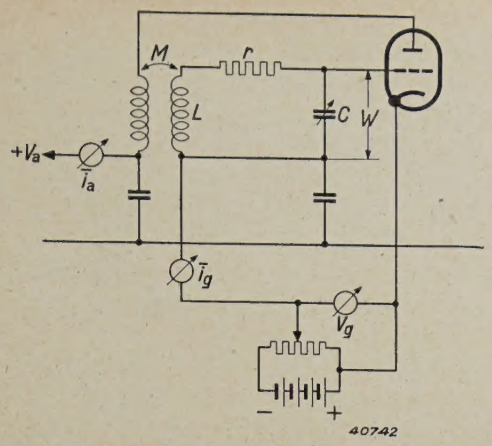

Fig. 1. Customary oscillator connections with triode. On the oscillation circuit, consisting of L, C and r, the A.C. voltage W is developed, M is the coefficient of mutual induction between the back-coupling coil in the anode connection and the circuit self-induction L. On this arrangement the grid of the triode receives a permanently fixed D.C. voltage by means of a potentiometer.

also given, as well as the static grid-current characteristic: i_{g_0} as a function of V_g.

The vertical line on the left indicates that when the negative grid voltage is raised above 40 V oscillation ceases. The anode current then falls to zero and the negative grid voltage V_g must be reduced to 4 V to obtain oscillation once more. For this purpose it is necessary that some anode current i_{g_0} should begin to flow in the non-oscillating state, so that the slope of the valve will reach the minimum value necessary for oscillation.

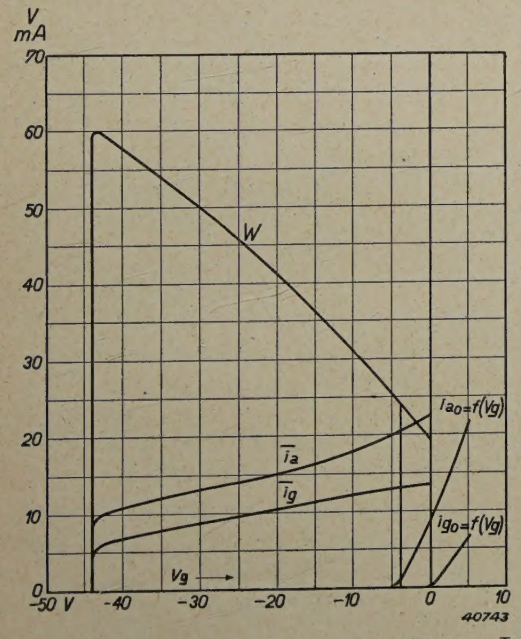

Fig. 2. Characteristics of a triode oscillator. In this diagram the behaviour is represented for a given case of the A.C. voltage W (peak value), the average anode current i_a and the average grid current i_g upon variation of the potentiometer voltage in fig. 1. The oscillation is seen to break off at a definite negative bias (about 44 volts).

We shall not attempt to explain the behaviour of $\bar{i}_a$, $\bar{i}_g$ and W in fig. 2 in detail. We shall only go more deeply into the character of the variation of these quantities in the neigbourhood of the maximum negative grid bias. It is remarkable here that W always continues to increase with increasing grid bias, except for a slight fall just before the interruption of the oscillation; $\bar{i}_a$ and $\bar{i}_g$, on the contrary, become steadily smaller with increasing grid bias. At the grid bias at which the interruption takes place they have not yet, however, decreased to zero, but still have finite values.

These facts may be explained as follows. As may be seen from the static characteristic, the valve is working in a region of grid voltages where the anode current would be zero if there were no A.C. voltage present on the oscillation circuit. In order to cause an anode current to flow there must be a certain A.C. voltage and the amplitude of this required vol age increases with the negative control-grid voltage. Due to this oscillation a finite amount of energy is dissipated in the oscillation circuit; the maintenance of the oscillation thus requires a finite anode current. The fact that the grid current thereby also remains finite will appear from the following considerations.

The oscillator with grid resistance and grid condenser

We now alter the oscillator diagram by substituting for the potentiometer a grid resistance R (often called leakage resistance) shunted by a condenser K, which we shall call the grid condenser. We then obtain the diagram of *fig. 3*. The grid D.C. voltage V_g here is thus formed by the average grid current i_g causing a voltage drop over the resistance R. The condenser K, acts more or less as a buffer, which transforms the irregular current impulses from the grid into a uniform current through the resistance. The current impulses from the grid are thus taken up by K, while a fairly

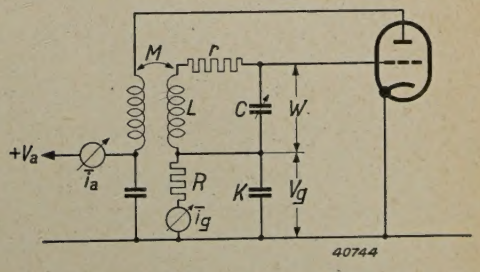

Fig. 3. Oscillator connections in which the fixed potentiometer voltage of fig. 1 is replaced by a variable bias obtained by means of a grid condenser and leakage resistance.

uniform direct current flows through R, which current maintains the level of the negative voltage of K. It is advisable to have this process clearly in mind, especially in connection with the discussion to follow. In the oscillator diagram of fig. 3 we can now obtain different grid voltages V_g by varying the value of the grid resistance R. We shall set about this systematically and vary R continuously from the value zero to the value infinity. We then include at the same time the average values of the anode and grid current i_a and i_j, and, as in the case of fig. 1, the peak value W of the oscillator voltage.

The result of this is reproduced in *fig. 4.*

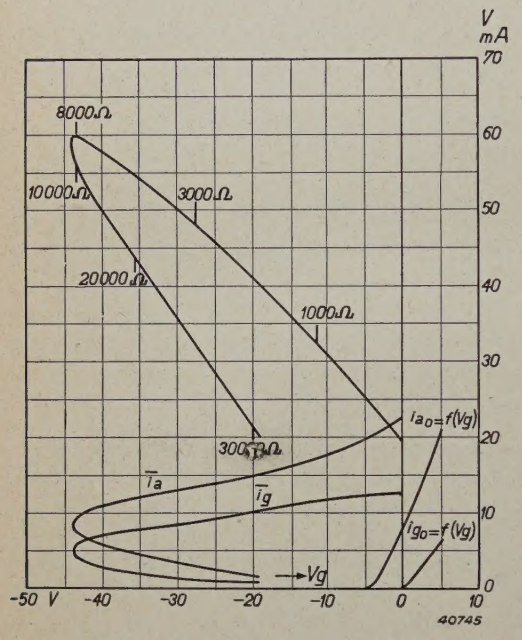

Fig. 4. Characteristics of a triode oscillator according to the diagram of fig. 3. It may be seen that the same curves are obtained as in fig. 2, which represented the behaviour of the circuit of fig. 1, but with an extension which returns to smaller values of V_g.

V_g is here determined, therefore, by taking the product of i_g and R. As may be seen from fig. 4, we first obtain the curves of fig. 2 once more, *while for values of R greater than the value which corresponds to the point where oscillation breaks off in fig. 2, we find an extension of the curves which returns to smaller values of* V_g. As functions of R the A.C. voltage W and the negative grid voltage Vg thus exhibit a pronounced maximum, while i_a and i_g decrease steadily.

Due to this receding character of the curves two adjustments of the oscillator are possible within a given interval for every value of the grid voltage, one of which can be realized with the help of a battery or a leakage resistance smaller than a certain value (9000 Ω in the case in question), while the other is obtained with a leakage resistance larger than 9000 Ω. These two possibilities of adjustment are especially different with respect to the damping of the oscillation circuit due to grid current. If, for example, the two adjustments are considered in the diagram for a negative grid voltage of 20 V, a grid current of $i_j = 10$ mA is found for an adjustment to the upper branch of the curves, while on the returning branch at the same grid voltage a grid current of less than 1 mA is obtained.

The fact that the grid current here is so small is in agreement with the fact that the oscillator amplitude W is only slightly larger than the negative grid bias (namely, $W = 21$ V, when $V_g = -20$ V), so that the total grid voltage swings only slightly into the region of positive values. In the case of the adjustment obtained with the help of a battery, as we have seen, much larger grid currents occur, so that much more energy is necessary to maintain the oscillation. The anode current i_a on the upper branch is then much larger than on the lower branch for a given value of W.

We shall now attempt to explain this double possibility of adjustment on the basis of a diagram. It will then become evident at the same time why with a fixed bias in fig. 1 we could not find the adjustments on the receding part of the curves in fig. 4, and why regular oscillation is no longer possible after a certain value of the leakage resistance R.

Effective slope, required slope and grid current damping

In the discussion of the oscillator with fixed bias (fig. 2) it was pointed out that at grid voltages greater than 4 V negative (*i.e.* to the left of the vertical line) an oscillation is no longer built up automatically when it has been interrupted by some cause or other. For the sake of brevity we shall call this region of the grid bias the C-region, the region to the right of it the A-region, to correspond with the terminology customary in the case of amplifiers : class C and class A.

Oscillation with the grid D.C. voltage in the C-region is thus only possible when the grid voltage is first taken in the A-region and subsequently shifted to the C-region. In the case of fig. 1 this was done by the variation of a potentiometer, in the connections of fig. 3 this process occurs automatically due to the fact that with increasing oscillator voltage the negative grid voltage increases because of the grid current.

The way in which the oscillation is maintained when the grid D.C. voltage lies in the C-region can be understood in the following

way. We assume a constant grid bias of for instance 30 V in fig. 2, and desire to know how the effective slope of the triode depends upon the grid A.C. voltage W. By the effective slope S is then meant the quotient of the first harmonic in the anode current and the grid A.C. voltage (assumed to be sinusoidal). The way in which S_{eff} behaves as a function of W is sketched in *fig. 5*.

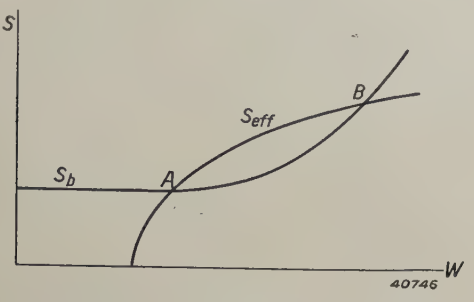

Fig. 5. The slope S_b necessary for oscillation and the effective slope S_{eff} as functions of the A.C. voltage W at a given negative grid D.C. voltage. In the case of this diagram the latter is chosen so large that the valve is in the overbiased state (C-region). For small values of the A.C. voltage W the effective slope is zero.

For small values of W, as long as the peaks of the A.C. voltage do not yet enter the anode-current region of the grid voltage, S_{eff} is zero. S_{eff} then takes on a certain value which grows gradually in order finally to reach a maximum value and then to decrease again if the triode exhibits saturation phenomena (this is not indicated in fig. 5).

Further, it is indicated in fig. 5 how the slope r e q u i r e d for oscillation varies as a function of W. This required slope S_b is constant at first, since it is determined by the (constant) resistance. If, however, the A.C. voltage W becomes so large that grid current begins to flow, the oscillation circuit is damped by this grid current and the required slope increases. This explains the shape of curve S_b in fig. 5.

The curves for S_b and S_{eff} in fig. 5 in the case of the behaviour described will in general intersect twice (or not at all). At these points of intersection A and B the required slope is equal to the effective slope, and the oscillator voltage could thus adjust itself to the corresponding values of W.

It is now easy to understand that in the case of the circuit with fixed bias (fig. 1) the oscillator voltage will adjust itself at point B. The point A is an unstable adjustment. If the A.C. voltage becomes slightly greater at point A for example, the effective slope increases more rapidly than the required slope, so that there is an excess of exciting forces over the damping forces, with the result that the A.C. voltage will increase still more and finally reach the operating point B which, it is easy to see, forms a stable adjustment of the oscillator. Conversely, with a slightly too small A.C. voltage the oscillator would cease to generate. We thus reach the result that upon the use of a fixed grid bias, of the two possibilities of adjustment A and B, the adjustment with the larger oscillator amplitude will be chosen.

If we now pass on to the oscillator connections with grid resistance we can explain the character of the curves reproduced in fig. 4 by assuming that on the receding branch of these curves we are concerned with an adjustment of the nature of point A in fig. 5. The question then naturally arises as to the way in which this adjustment just described as unstable has now obtained stability.

Before answering this question, however, we shall consider the stability as a given property and ask what happens to the point of intersection A when the leakage resistance R is made steadily larger.

By changing R the grid voltage is altered and this changes the shape of the curves S_b and S_{eff}, while at the same time there will be a relative displacement of the curves. The highest negative bias which can be realized with the help of a leakage resistance amounts to about 44 V; at this voltage the curves S_b and S_{eff} lie so far apart that instead of two points of intersection there is only point of contact between the two curves [3]).

With decreasing value of the negative bias curve S_{eff} will be displaced towards the left, whereupon the point of intersection A is also displaced towards the left, so that the oscillator amplitude W becomes smaller. If W is drawn as a function of V_g the relation represented in *fig. 6* is obtained for the oscillator under consideration.

In order to draw conclusions from this about the behaviour of the oscillator, the quantity $W - V_g$ is also plotted in fig. 6 as a function of V_g. In the state of adjustment actually reached this quantity must always be larger than zero. If this were not so no grid current would flow, so that the grid voltage acting on the leakage resistance R could not continue to be maintained. This shows that with every leakage resistance the negative grid bias must adjust itself to a value which lies to the left of V in

[3]) If a battery is used for the excitation of the grid bias instead of a leakage resistance, the bias can of course also be made greater than 44 V. The point of intersection or contact, as the case may be, of the curves then disappears entirely, with the result that the oscillation is broken off (see fig. 2).

fig. 6 (in the example investigated about 15 V) and which approaches the limit V_∞ with increasing value of R.

The variation of W as a function of V_g reproduced is actually nothing else but the receding branch of the curve for W in fig. 4. In that case it was impossible to record the whole curve, since upon an enlargement of the leakage resistance beyond about 30 000 Ω the stability at the point of intersection is lost and blocking occurs. The receding branch therefore does not continue to $V_g = V_\infty = -15$ V, but ends already at —19 V.

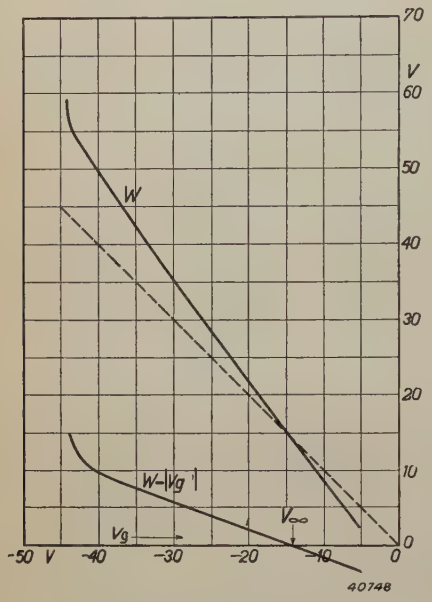

Fig. 6. If the diagram of fig. 5 is drawn for different values of V_g, the abscissa W of the point of intersection A takes on different values. The above curve gives this value of W as a function of V_g. Below is the difference between W and the absolute value of V_g. Stationary states are only possible when $W-|V_g|>0$, *i.e.* for grid voltages to the left of V_∞.

The stabilizing action of grid condenser and leakage resistance

Until now we have considered only those oscillator adjustments at which the negative grid voltage was so high that in the absence of a grid A.C. voltage only very little or no anode current would flow (C-region). The essential point in this is that the effective slope increases with increasing A.C. voltage W (see fig. 5).

If, however, we choose the grid D.C. voltage less strongly negative, so that an anode current already flows even without grid A.C. voltage, the slope then decreases with high A.C. voltage, due to the fact that a continually larger part of the grid A.C. voltage varies in a region with low anode current or an anode current of zero. In this way we obtain the diagram of *fig. 7* instead of that of fig. 5. We then have only one point of intersection of the curves for the required and the effective slope and this of itself already represents a stable adjustment. Thus when the grid bias lies in the A-

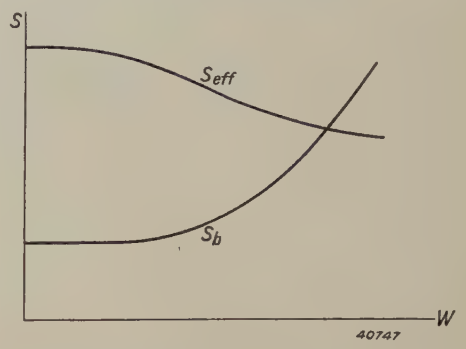

Fig. 7. Diagram analogous to fig. 5. The negative grid D.C. voltage, however, is chosen much lower, so that maximum slope occurs at low values of the A.C. voltage W (A-region).

region there is no essential difference between oscillation with fixed bias and oscillation with grid condenser and leakage resistance. Therefore the discussion of adjustments with the grid D.C. voltage in the C-region is sufficient.

The explanation of the fact that the unstable adjustment A of fig. 5 may become stable upon the use of an R-C circuit is the following. Let us again assume a slight deviation, for instance an increase in the A.C. voltage W. In the first instance this causes an increase of the effective slope, which would lead to a further increase of W. On the other hand a larger value of W means more grid current and, as a result, an increase in the negative grid voltage. As a result of this, however, the slope decreases again, so that the unstable growth of the oscillator amplitude is opposed.

It is now the question whether such a reaction may have as a result that an adjustment which is of itself unstable becomes stable. It may reasonably be expected that this will depend upon the speed with which the reaction takes place and thus on the magnitude of K. When the condenser K is made so large that upon short-lived fluctuations of the working state it acts practically like a battery with constant voltage, there is no question of a stabilizing influence.

In the opposite case of a very small value of the capacity K, on the other hand, the stability of the working state is easily demonstrated. In this case we may assume that every change in the oscillator voltage W is immediately accompanied by a certain change in the bias V_g. The equilibrium between the required slope S_b and the slope actually present S_{eff} can now be described by a diagram analogous to that of fig. 5 or fig. 7, but with the difference that the grid D.C. voltage does not have a constant

value but at each oscillator amplitude W is equal to the value which is automatically adjusted for this. With increasing value of W we then find a regularly decreasing value of S_{eff}, since the negative grid voltage becomes steadily greater while the peaks of the A.C. voltage extend only relatively slightly into the grid current region. The required slope S_b is now practically constant, since the grid current damping is slight and, moreover, almost constant.

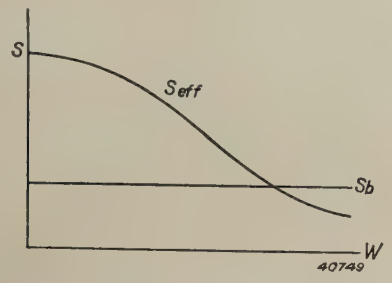

Fig. 8. Diagram analogous to fig. 5 and fig. 7. Now, however, the grid D.C. voltage is not considered to be constant, but a function of the A.C. voltage W, namely that D.C. voltage which is automatically attained by means of the grid condenser and leakage resistance at each corresponding value of W.

We thus obtain the diagram for S_b and S_{eff} which is shown in *fig. 8* and which qualitatively is analogous to fig. 7. Just as in fig. 7, we may also conclude that the point of intersection represents a stable state. It must be repeated that the stability of the adjustment is not yet proved for the general case by this consideration, since the diagram of fig. 8 is only correct when at each value of W the grid voltage is immediately equal to the value which would be reached in the course of time. If this adjustment proceeds too slowly, a state on the receding branch of the curves of fig. 3 finally becomes labile. Fig. 8 does indeed prove that at a given value of R there is only one possible stationary adjustment. This single adjustment can therefore still be unstable.

For the present we may summarize the foregoing discussion in the form of the following conclusion:

When in the case of an oscillator with grid condenser and leakage resistance the back-coupling is increased so much that the grid D.C. voltage lies in the C-region (see the preceding definition), with the customary large values of the leakage resistance the adjustment of the oscillator is one which would be unstable with a fixed grid voltage, but which has become stable due to the action of the grid condenser and leakage resistance. If this stabilizing action is insufficient, due for instance to the fact that the grid condenser has been chosen too large, the only possible adjustment becomes unstable and blocking occurs.

A careful study of this "wild" oscillation or blocking falls outside the scope of this article, but its actual cause will have become sufficiently clear from the foregoing. In a following article we shall supplement this qualitative discussion by a quantitative treatment of the problem of stability, in which at the same time more light will be shed on the behaviour of the oscillator in the unstable state. In addition the measures will also be studied which may be taken against blocking.

THE TEXTURE OF NICKEL-IRON STRIP

by J. F. H. CUSTERS.

620.18 : 669.15.24

After a discussion of the method of investigation and graphical representation of texture in a previous article, the texture of nickel-iron strip for loading coils is here discussed in several states of working as a first example of the study of textures.

Many properties of polycrystalline metals are considerably affected by their so-called preferred orientation or texture, *i.e.* by the way in which the crystallographic axis directions of the single-crystalline grains of which the metal is built up are oriented. In a previous article which appeared in this periodical [1]) it was explained how the texture of a piece of metal can be determined by means of X-rays and how it can then be represented graphically. In this article we shall consider as an example the texture of nickel-iron strip in various conditions of working. Nickel-iron strip which has undergone certain manipulations and heat treatments has, as previously mentioned in this periodical, an important technical application as core material for loading coils [2]).

[1]) J. F. H. Custers, A consideration of the texture of metals, Philips Techn. Rev. **7**, 13, 1942.

[2]) J. L. Snoek, Magnetic cores for loading coils, Philips Techn. Rev. **2**, 77, 1937. See also W. G. Burgers, Philips Techn. Rev. **2**, 93, 1937. Further: G. W. Rathenau and L. J. Snoek, Physica **8**, 555, 1941.

The manipulations referred to are briefly the following: Nickel and iron are alloyed and an ingot with coarse-grained structure is obtained. By several deformation and heating processes a fairly fine-grained strip is obtained from this ingot, which is about 1 cm thick and exhibits no texture at all. The strip is then further cold-rolled in many steps until the thickness of the strip is finally only 0.1 mm. As a result of this rolling the strip has undergone enormous deformations and has become even more fine-grained. Many properties have been very much altered compared with the original strip, which was 100 times as thick. The hardness has increased considerably, the resistance to bending and folding has been changed not only in value but also in dependence on the direction, while the tensile strength has also undergone similar changes.

Before the strip is ready for use it must still be subjected to two operations, namely heating and rolling once more. It is, however, interesting, and it was found also to be of practical importance, to make an investigation of the texture of the material in this intermediate stage of working. Upon projection of the reference sphere on a plane parallel to the plane of the strip, the pole figure given in *fig. 1* is then found for the cube planes of the crystal lattice.

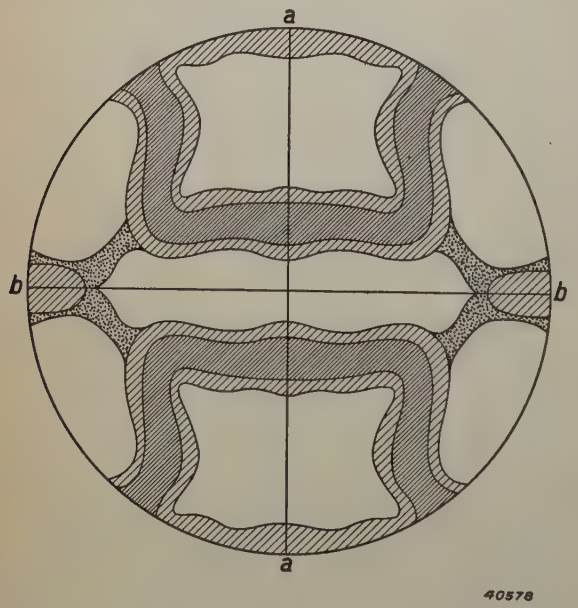

Fig. 1. Pole figure for the cube planes in the case of the rolling texture of nickel-iron strip. The projection plane of the pole figure (plane of the drawing) is parallel to the plane of the strip; *a-a* is the direction of rolling. The blackened parts represent the statistical distribution of the directions of the normals to the cube planes in all the cristal grains of the strip. The density of "occupation" is here indicated in four steps. The closely-spaced shading indicates the greatest, the wide shading a less density, the dots the smallest density of occupation which can be observed. The white parts are unoccupied.

As was described in the article refered to in[1]), a texture is represented graphically by considering a certain kind of lattice planes — for instance the cube planes — of the piece of metal, drawing for each crsytal grain the normals to those lattice planes and allowing them to pierce a sphere drawn about the specimen, the reference sphere. The more or less pronounced pattern of points obtained on the sphere, which furnishes an image of the texture of the piece of metal, is represented graphically, by stereographic projection of the reference sphere, in a pole figure, In the case of a given object with an unknown texture the pole figure can be determined by means of a series of X-ray diffraction photographs with monochromatic radiation which are taken in a series of slightly rotated positions of the object under investigation. In *fig.* 2 such a series of photographs is given of the rolled nickel-iron strip, whereby the beam of X-rays was directed perpendicular to the direction of rolling of the strip and perpendicular to the surface of the film, while the strip, starting from a position parallel to the surface of the film, was turned 5° farther each time around the direction of rolling. On each photograph a heavy blackening can be seen (white on the positive) of certain parts of the different Debije-Scherrer circles, which circles correspond to the different lattice planes of the crystal lattice. If in all the photographs we consider only the circle for the cube planes — in fig. 2 this is in each case the second circle from the centre, the first is that for the octahedron planes — the pole figure can be constructed from the blackened segments in the successive exposures in the manner previously described.

The pole figure in fig. 1 is closely related to that found for other metals after rolling which, like nickel-iron, crystallize in a face-centred cubic lattice, aluminium and copper for example. It is therefore called a "rolling texture". The preferred positions which this texture involves and about which the separate grains are arranged with a certain scattering can be described in this case in different ways. A good approximation is obtained when the two positions of the cube faces indicated in *fig. 3* by a model of a cube with respect to the direction of rolling *a-a* are considered preferred positions [3]). To these positions correspond the poles drawn in *fig. 4*, and this shows that upon the assumption of a certain scattering in the actual positions of the grains about two ideal preferred positions, so that more or less extensive regions occur in the pole figure instead of sharp points, the pole figure of fig. 1 can be obtained. According to our own experience, however, considering the phenomena which occur upon heating the strip[4]), it is better to consider the rolling texture as characterized by the preferred position indicated in *fig. 5*. The latter as well as the positions symmetrical to it in the strip are represented in the pole figure by the dots drawn in *fig. 6*, and it may be seen that upon the assumption

[3]) See Frhr. v. Göler und G. Sachs, Z. Phys. **41**, 873, 1927.

[4]) See J. F. H. Custers and G. W. Rathenau Recrystallization in rolled nickel-iron, Physica **8**, 759-770, 1941 and J. F. H. Custers, Über die (111)-Reflexe im gewalzten und rekristallisierten Nickeleisen, Physica **8**, 771-788, 1941.

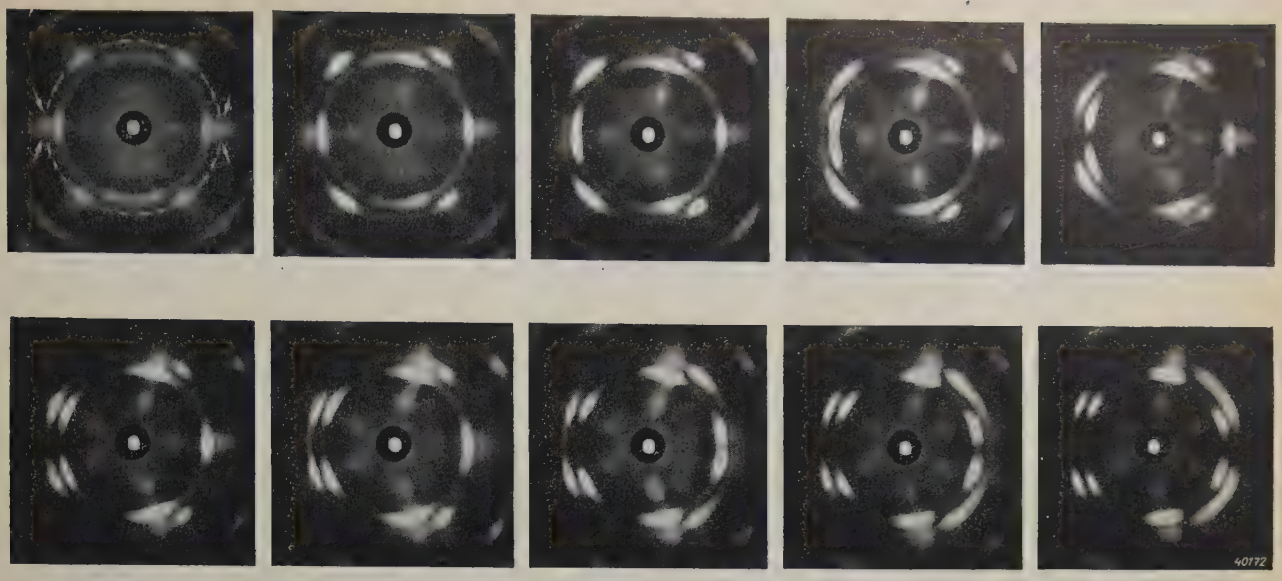

Fig. 2. X-ray diffraction photographs of rolled nickel-iron strip. In the first exposure the plane of the strip was parallel to the plane of the film, in the following exposures the strip was turned 5° farther in each case about the direction of rolling (direction from top to bottom). The blackened parts of the different Debije-Scherrer circles indicate where the so-called reflection circle which corresponds to each position of the strip (see the article referred to in footnote [1])) passes through regions on the reference sphere of the piece of metal which are covered with points of intersection. If in all the exposures the Debye-Scherrer circle for the cube planes (indicated by a dotted circle in the first photograph) is considered, the pole figure of the cube planes given in fig. 1 can be derived from the whole series. The spots indicated in the first exposure by arrows, which are also visible in part of the following exposures, are due to grains in the so-called cube position.

here also of a certain scattering the pole figure actually found for the rolling texture is satisfactorily approximated. The position indicated in fig. 5 is of itself rather difficult to describe in words [5]). It must, however, be kept in mind that for describing the texture it is not actually necessary to be able to give

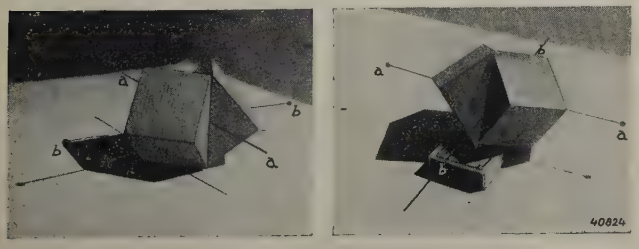

Fig. 3. According to Sachs [3]) the rolling texture of nickel-rion strip may be considered as originating from the two ideal preferred positions of the cube planes here represented in a model with respect to the direction of rolling *a-a* and the transverse direction *b-b* of the strip.

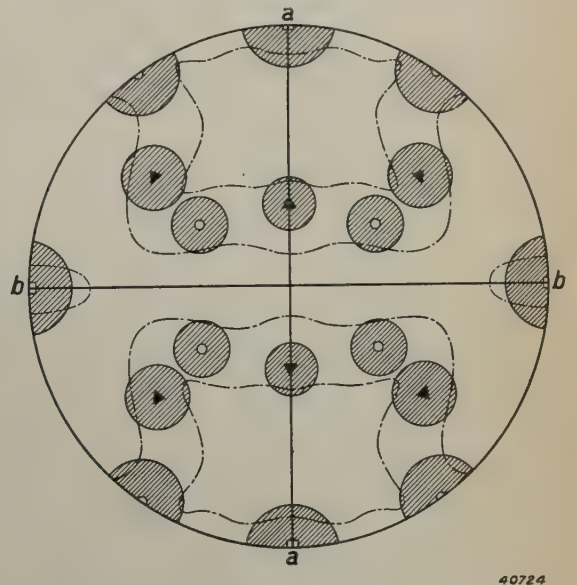

Fig. 4. The poles of the positions of the cube planes shown in fig. 3 form such a pattern in the pole figure that, with the assumption of a certain scattering around these positions, the pole figure of the rolling texture (fig. 1) is quite closely approached. The poles indicated by small triangles belong to the left-hand position in fig. 3, the small circles to the right-hand position. Around each pole a circle is drawn which corresponds to a scattering of 10° around the position in question. The rectangles with their circles do not belong to the rolling texture proper, but to the cube position.

[5]) To do this one must begin with a crystal whose three axes coincide with the direction of rolling, the direction of the normal and the transverse direction of the strip perpendicular to the first two directions, Let a twin be formed on such a crystal (in the so-called cube position), *i.e.* in the growth of one of the octahedron planes the crystal "by mistake" builds up an atomic layer in hexagonal closest packing instead of in cubic closest packing, then proceeding with cubic closest packing again the crystal is thereby rotated 60° about the normal to the octahedron plane. The preferred position in question now occurs when this twin is further rotated through a small angle (about 8°) about the normal mentioned.

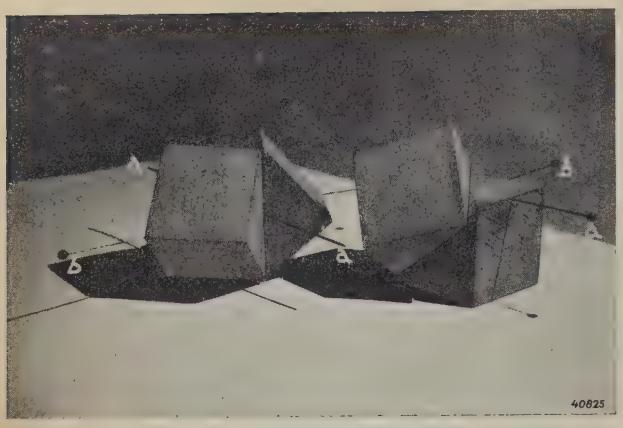

Fig. 5. According to our own investigations the rolling texture can best be described by the preferred position of the cube planes here illustrated.

names to the "ideal" preferred positions ; the positions in which the grains actually stand and the statistical distribution of their positions is indeed already completely represented by the experimentally determined pole figures. The recognition of the ideal preferred positions is only important when it is desired to make a further investigation of the mechanism of the occurrence of a given texture, or when a relation is sought on the basis of crystallographic data between the texture and quantitative differences in properties of different materials. In this respect, however, little can yet be said about the rolling texture.

We have already stated that the rolled strip is not yet ready for use, *i.e.* the rolling texture is not yet the desired texture. If the strip is now heated to a sufficiently high temperature and the texture then examined anew, a complete change is found to have taken place. The grains which we now encounter in the strip are much larger than in the rolled strip and nearly all of them are in such positions that the axis directions coincide with the rolling direction, the direction of the normal and with the transverse direction of the strip respectively (*fig. 7*). The scattering of the positions of the grains about this so-called cube position is relatively slight, so that the strip may be considered almost as a single nickel-iron crystal. The appearance of this new texture must be due to the growth of certain crystal nuclei thanks to the thermal agitation of the atoms (recrystallization). Due to the rolling, germs have indeed been formed in the nickel-iron strip which are in the cube orientation and which may function as nuclei for recrystallization. This may clearly be seen in the photographs of fig. 2 : the Debye-Scherrer circle for the

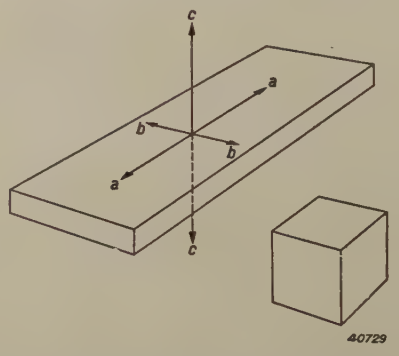

Fig. 7. In the so-called cube position the three cube axes of the nickel-iron crystals are parallel to direction of rolling *a-a*, transverse direction *b-b* and direction normal to the strip *c-c*, respectively.

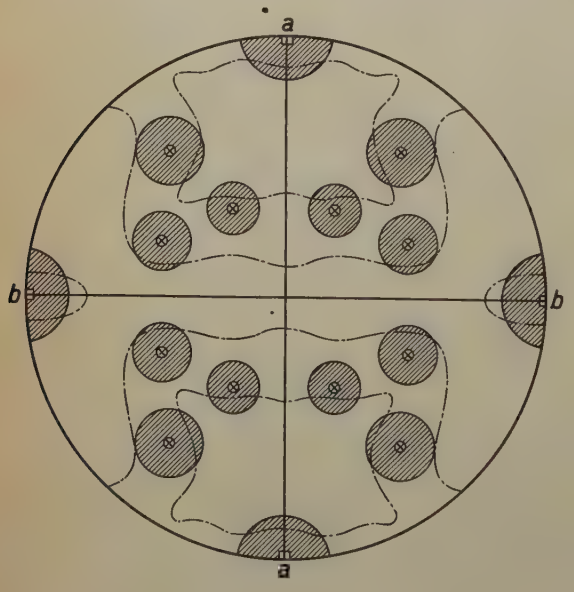

Fig. 6. The poles of the cube planes in the position of fig. 5, as well as the corresponding symmetrical positions, together with their circles of scattering, coincide satisfactorily with the pattern of the pole figure fig. 1.

cube planes in the first five or six exposures in which the strip is approximately parallel to the film contains a visible blackening at the points of intersection with the horizontal diameter of the circle, which is what occurs in the case of grains in the cube position. The reason why germs in the cube orientation have such a capacity for growth that in the recrystallization they consume all the grains not in this position, is not yet fully explained ; there is probably some connection with the magnitude of the energy of deformation which is stored up in the grains in the rolling process. Whatever the case may be, the cube orientation resulting from the recrystallization is found to be very sharp, as is shown by the X-ray diffraction photographs *fig. 8* and the pole figure *fig. 9* obtained from them. At the same time the properties have also changed compared with those of the rolling texture ; for example the material has become much softer again. In particular, however, it is found to begin to exhibit a property which is especially desirable for its use in loading coil

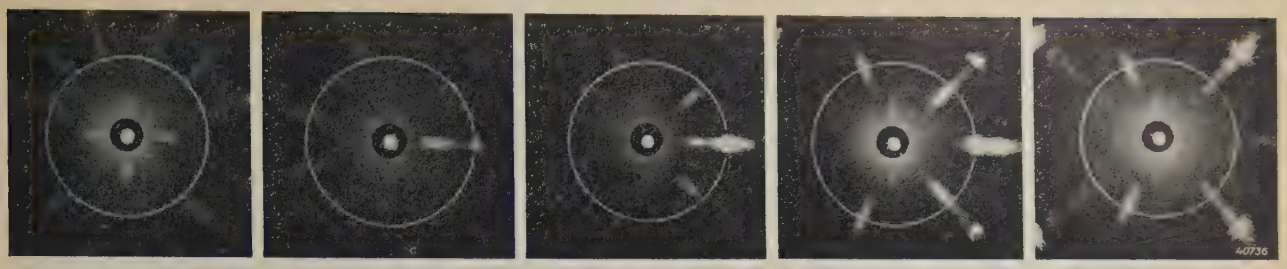

Fig. 8. X-ray diffraction photographs of recrystallized nickel-iron strip taken in the same way as in fig. 2. The texture is entirely changed : almost all the grains are in the cube position, as is evident from the intenseblacken ing on the circle of the cube planes in the third and fourth exposures of the rotated strip. The fact that in the first exposures (perpendicular incidence of the X-rays) the blackenings of the cube orientation, which were indicated in fig. 2 with arrows, are lacking, indicates precisely that the texture is very sharp : in the case of the position of 0° the reflection circle does not yet pass through the thickly occupied regions in the reference sphere and only moves through their middle at the position from about 5 to 15°, while with the less sharply pronounced cube position of fig. 2 the blackened regions on the reference sphere are so extensive that at the position of 0° the reflection circle already passes through them.

and which appears fully after a further final operation, namely rolling out to about half the thickness. The strip then has a strong mono-

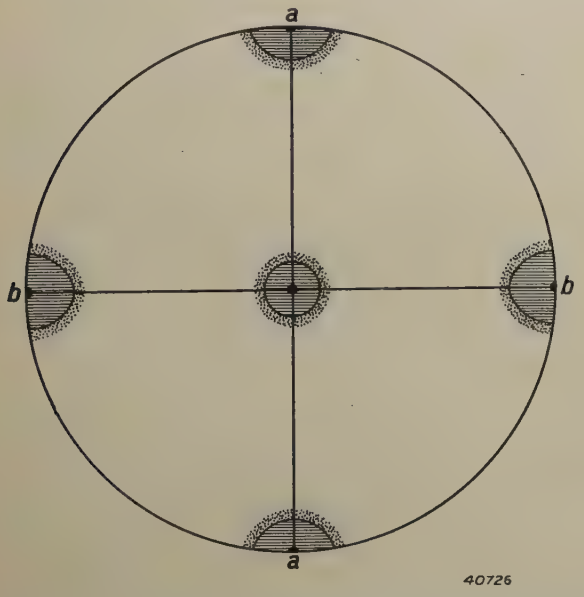

Fig. 9. Pole figure for the cube planes derived from fig. 8. The texture (cube position texture) is very sharp, the material behaving almost like a single crystal.

axial magnetic anisotropy : it can be magnetized with much more difficulty (*i.e.* only by stronger fields) in the direction of length (and that of the normal) than in the transverse direction. In consequence of this, with suitable assembly in the self-induction coil, the hysteresis and the so-called instability of the core, which are undesirable for loading colis, can be kept very low (see the first article referred to in footnote [2])).

The part actually played by the last operation in the appearance of the strong magnetic anisotropy has not yet been explained. The texture is not thereby appreciably changed, as may be seen upon comparison of the two X-ray diffracton photographs of *fig. 10*. The scattering in the positions of the grains about the cube position has only become somewhat greater.

Although it may be seen from the above that in this case — and in other cases it is often the same — there are still many questions to be answered, it will, nevertheless, have become clear that theoretically and practically it may be of importance in working a metal to study its texture at different stages in the proceedings and to attempt to connect the texture with the properties of the material.

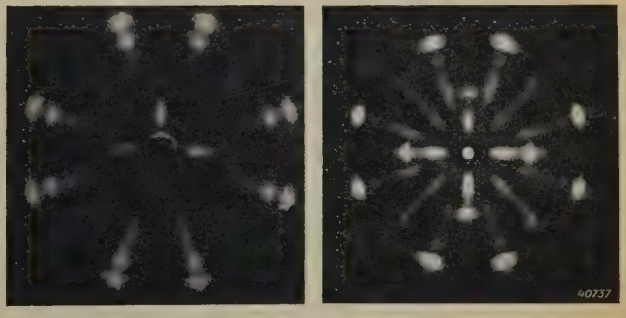

Fig. 10. After the last operation (final rolling) the texture of the strip is still the same as after the recrystallization, but somewhat less sharp, as may be seen upon comparison of these exposures made with perpendicular incidence: left before, right after rolling. The left-band exposure is in fact identical with the first of fig. 8. Due to the greater scattering after rolling, the blackenings for the cube orientation are already visible upon perpendicular incidence of the X-rays.

A RECORDING APPARATUS FOR THE ANALYSIS OF THE FREQUENCY OF RAPIDLY VARYING SOUNDS

by H. G. BELJERS.

534.441.2

By the use of a series of band filters whose transmission regions are distributed over the whole range of acoustic frequencies an accurate and rapid analysis of the frequency of speech and other rapidly varying sounds is possible. An apparatus based upon this principle is described here, with which the Fourier spectrum of the sound to be investigated is made directly visible on the screen of an electron ray oscillograph, so that the variations of the spectrum can be filmed. The properties of the apparatus, especially the resolving power and recording speed attainable are discussed, as well as a number of particulars of construction and use. In conclusion several spectrograms of vowels filmed with the apparatus are reproduced as examples of its use, and they are briefly discussed.

In the case of electro-acoustic apparatus for the transmission of speech or music it is customary to describe the behaviour of the whole or of the separate elements by the way in which they react to sinusoidal oscillations of different frequency. This custom is based upon the fact that every sound vibration can be resolved into a number of sinusoidal components (Fourier components), so that from the frequency characteristics of an element (amplifier, cable or the like) it is possible to deduce immediately the form in which the complex vibration will be transmitted.

There are many numerical, graphic and instrumental methods for the separation of a vibration into its Fourier components, *i.e.* methods of harmonic analysis. For the most part, however, these methods are based upon the use of functions which are given in the form of a diagram or a table. If, therefore, it is desired to analyse sound vibrations by these methods, the sound vibrations must first be recorded. Moreover, the frequency spectrum of sound vibrations, that of speech for example, continually changes, and it is often just these changes in which we are interested. In order to investigate these changes a large number of strips of the recorded sound would each have to be analysed separately, which is a very laborious method scarcely deserving practical consideration.

With these objections in view special methods of separation have been developed for electro-acoustics which correspond better to the existing requirements and possibilities in this field.

A very obvious method is to make use of a band filter as analysing element. If by means of a microphone the sound vibration is converted into an electrical A.C. voltage and this is fed successively to a number of band filters with different transmission regions, then from the occurrence or absence of an output signal it can be deduced in what frequency regions components of the vibration being investigated lie, and how strong they are. Obviously so many filters must be used that the desired fineness of structure of the whole acoustic spectrum is obtained.

In order to avoid the necessity of a large number of band filters, which make the apparatus complicated and expensive, the following device is usually employed. A sinusoidal voltage whose frequency can be continuously varied (auxiliary frequency), is fed, together with the signal to be investigated, to a mixing valve followed by which is a single band filter. If the difference frequency (or sum frequency) of the auxiliary frequency and one of the frequencies present in the signal falls exactly in the narrow transmission region of the band filter, an output signal is observed. From the values of the auxiliary frequency at which this occurs the Fourier spectrum of the signal can therefore be deduced.

Only one band filter is needed here, but two disadvantages are also involved: the measurement takes some time and as a result a fairly lengthy constancy of the voltage to be investigated is required. Therefore the auxiliary frequency method can indeed be used, for example, for determining the deformation which a given constant input signal undergoes in an apparatus, but not for the analysis of speech or other rapidly varying sound.

For an analysis of these sounds, therefore, recourse must be had to the fundamentally simpler method in which separate band filters are used for the different components of band filters required.

Equipped with such a set of analysing elements, it is now also possible to make the Fourier spectra visible directly in a simple way. For this purpose the outputs of the whole series of band filters are connected successively with an electron ray oscillograph by means of a rapidly rotating switch. By means of suitable connections the spectrum of the sound to be analysed can then be observed directly on the fluorescent screen, and its variations seen or recorded on a film.

An apparatus working on this principle and constructed in this laboratory will be described in this article [1]), while in conclusion some results obtained with the apparatus will be dealt with.

Description of the apparatus

In *fig. 1* the whole apparatus is shown diagrammatically. It contains 79 band filters (F), whose successively scanned by a rotating switch E_1. In this way the rectified voltage of each band filter in turn, which voltage is a measure of the corresponding component of the Fourier spectrum, is fed to the vertical deflection plates of a cathode-ray oscillograph (the elements G and M in fig. 1 will be disregarded for the present). At the same time a D.C. voltage in-

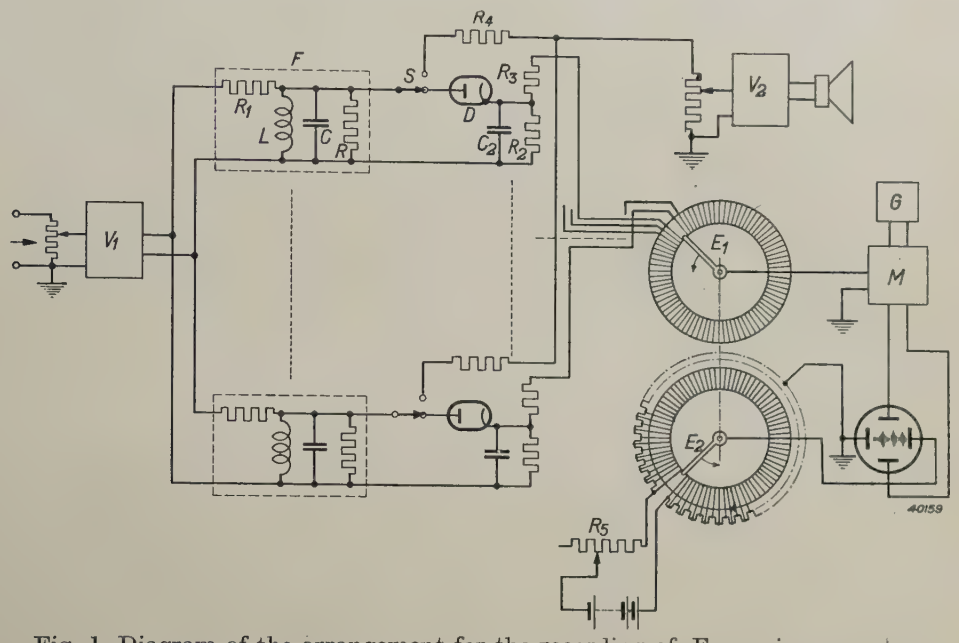

Fig. 1. Diagram of the arrangement for the recording of Fourier spectra. The sound to be analysed reaches the inputs of the 79 band filters *via* the pre-amplifier V_1; the part of the signal transmitted by each band filter is rectified with a diode D and fed *via* the rotating switch E_1 to the modulator M, which supplies a modulated carrier wave of high frequency to the vertical deflection plates of an electron-ray oscillograph. With the rotating switch E_2 a D.C. voltage increasing in steps is fed at the same time to the horizontal deflection plates. The length of the spectrum which appears in this way on the oscillograph screen is regulated with R_5; V_2 is a monitor amplifier which can be connected *via* resistances R_4 by 79 switches S to the output of each band filter.

transmission regions are distributed over the range of frequencies from 90 to 8000 c/s. The signal to be investigated is fed to the inputs of all the band filters connected in parallel. Since each filter can only transmit a very small part of the energy of the signal and the output voltage of each filter must, nevertheless, project sufficiently above the ordinary level of interference, the signal is amplified to the necessary level (4 W) in the pre-amplifier V_1, which because of inverse feed-back causes only a very slight distortion.

Behind each filter there is a diode rectifier which rectifies the output voltage of the filter. Each of these rectifiers is connected to one of 79 contacts on a collector, which contacts are

creasing in steps is fed to the horizontal deflection plates. This voltage is taken from 79 taps of a potentiometer by the switch E_2 rotating in synchronism with E_1. The potentiometer is supplied from a source of D.C. voltage. When this is done a definite horizontal deviation of the fluorescent spot on the oscillograph screen corresponds to each band filter, and therefore a frequency spectrum is traced directly on the screen.

If, as here described, the rectified output voltages of the band filters were fed directly to the oscillograph, the frequency spectrum would become visible in the form of a series of points. This would be difficult not only for the measuring of the frequency (*i.e.* the number of the band filter), but also for the measuring of the intensity of the components. Therefore an A.C. voltage of high frequency (50 kc/s) is actually fed to the vertical deflection plates, which frequency is excited by a generator G, and its

[1]) An acoustic spectrometer constructed by Siemens & Halske is based on the same principle (E. Freystadt, Z. techn. Phys. **16**, 533, 1935). In that apparatus, however, the division of the spectrum was less fine than in our case (namely 3 filters per octave).

amplitude is modulated in a modulator M with the rectified output voltages of the band filters. In this way vertical lines are traced on the fluorescent screen instead of separate points. In *fig. 2* such a spectrum is shown. This method also has the advantage that the apparatus could be made less sensitive to interferences. Behind the modulator there is another band filter which transmits only a narrow frequency region around the generator frequency of 50 kc/s. Interfering voltages of other (not too low) frequency, which may be induced on the connections between the rectifiers and the modulator, are filtered out in this way, while any distortion products and the noise are rendered practically harmless.

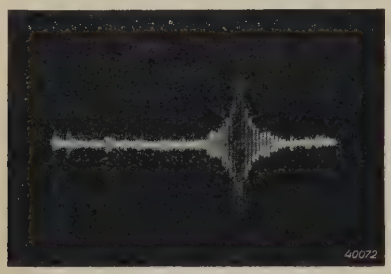

Fig. 2. Picture obtained on the oscillograph screen upon the application of a sinusoidal voltage to the input of the apparatus, when the frequency coincides with the resonance frequency of one of the filters.

The spectrum obtained on the screen, which in the case of speech for example continually varies, can be observed visually, or it can be photographed at short intervals on a moving film.

The action of the band filters can be checked by means of a monitor amplifier V_2 with loud speaker, which can be connected to each band filter in the place of the rectifier by means of a set of 79 switches S. By reversing several switches or whole groups of them the sound in different frequency regions can be heard and and the influence of the lack of certain frequencies on intelligibility can be studied.

After this brief description we shall now go into several important characteristics and structural details of the apparatus.

Resolving power and recording speed

It would be desirable to be able to determine exactly not only the frequency of each component but also the variations of its intensity with time, *i.e.* to be able to follow accurately the growth and disappearance of each component. The accuracy which can be attained here, however, is fundamentally limited by a kind of "relation of uncertainty". The frequency of a sinusoidal vibration can only be determined precisely when the vibration lasts for an infinite time. With shorter duration it is impossible to speak of one definite frequency of the vibration, but it must be ascribed to a spectrum of finite width, as appears from the theory of Fourier integrals. This width becomes greater the shorter the vibration lasts. Therefore the more rapidly a spectrum varies, the less sharp will the frequencies be determined.

In measuring, of course, only a section of finite duration of the vibration in question can be considered, so that even with an infinitely long vibration we cannot determine the spectrum perfectly sharply. But, moreover, the time interval must expressly be chosen short when rapid variations of a spectrum are to be observed; the organ reacting to the vibration (ear, filter or general measuring instrument) must "forget" again the preceding effects quickly enough. From a consideration of band filtersit is clear how in this case the antagonism mentioned occurs between the accuracy of the measurement of the frequency on the one hand (resolving power) and the recording speed on the other.

As indicated in fig. 1, the filters consist of single L-C circuits which are so damped by a resistance R in parallel that at resonance the impedance is 20 000 ohms. This is also the value of the preceding resistance R_1. The ratio a between output and input amplitude (transmission factor) of a vibration of any given frequency f with such a filter is

$$a = \frac{\mathrm{I}}{2 + jq\left[\left(\frac{f}{f_0}\right)^2 - 1\right]} \quad . \quad . \quad . \quad . \quad 1)$$

In this expression $f_0 = 1/2\pi\sqrt{LC}$ is the resonance frequency of the filter and $q = R/2\pi f_0 L$ is the so-called quality factor of the circuit (the loss resistance of the self-induction L is accounted for in the resistance R). The larger q, the steeper the resonance curve given by (1) falls away on each side of f_0 (*fig. 3*).

Let us suppose that a sinusoidal voltage is suddenly applied to the input of such a filter. In addition to a forced oscillation whose intensity can be calculated from (1), there then occurs a free oscillation with the frequency f_0 which gradually dies out according to

$$e^{-t/RC}.$$

The time $\tau = 2RC$ after which the intensity of the free oscillation has fallen by a factor $1/e$ is called the decay time of the filter. It will obviously be useless to measure the output voltage with a varying input A.C. voltage of the filter at intervals which are not at least equal to τ (preferably still much longer). Since the following is true:

$$\tau = 2RC = 2\frac{R}{2\pi f_0 L} \cdot 2\pi CLf_0 \cdot = \frac{q}{\pi f_0} \qquad (2)$$

the more rapidly it is desired to record, *i.e.* the smaller the decay time r is to be made, the smaller the quality factor q of the filters must be made, *i.e.* the flatter the resonance curves of the filters must be. Therefore the less accurately is the frequency of the transmitted signal determined.

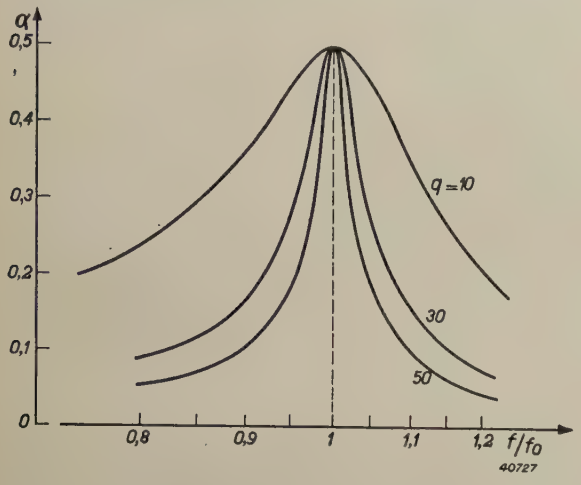

Fig. 3. Resonance curve $a(f)$ of the band filter for different values of the quality factor q.

From equation (2) it may at the same time be seen that at a given value of q the band filters have a shorter decay time for the high frequencies than for the low. For the high frequencies therefore a more rapid recording is possible than for the low frequencies. Since, when the whole spectrum is recorded with a single film, the same recording speed must be used for all frequencies, it would seem reasonable to construct all the filters with the same decay time, so that in the case of the filters for high frequencies it is possible to work with a high value of q, *i.e.* a sharp resonance curve and correspondingly great resolving power. We have not done this, however, because the sharper the resonance curves of the filters are made, the greater the chance that a Fourier component whose frequency lies just between the resonance frequencies of two neighbouring filters will remain unobserved. Since this must be avoided as far as possible the intervening regions between the filters must be made smaller, *i.e.* with a sharper resonance curve a larger number of filters is necessary.

In order not to be compelled to use too large a number of filters we chose the relatively small value of 32 for the quantity q. If we use a recording speed of 20 pictures per second, which will be sufficient for most investigations, the decay time will only be longer than the recording time for the filters with $f_0 < 32.20/\pi \approx 200$ c/s ; in the case of the lowest frequency with which we are concerned $f_0 = 90$ c/s, $\tau = 1/9$ s, so that rapid variations of the components in this neighbourhood will not be quite adequately brought out on the film. In practice, however, this is not a serious objection.

With the 79 filters already mentioned, whose resonance frequencies are distributed according to a geometrical series over the frequency range from 90 to 8000 c/s which is of importance for speech [2]) (there are then 12 filters to an octave and the frequency relation between two adjacent filters is therefore the same as between two adjacent notes on the piano (about 1.06)), it may be calculated according to equation (1) that the transmission factor of the filters and those frequencies f_m where two adjacent frequency curves intersect ($f_m/f_0 = 1.03$, see *fig. 4*), amounts to $\alpha = 1/2\sqrt{2}$. At resonance ($f = f_0$) $\alpha = 1/2$. Thus if a component lies just between two filters, both of these filters give a certain output signal from which the intensity of the component can be found by adding the squares. But when a component falls exactly at the resonance peak of a filter, several neighbouring filters to the left and right also give an output signal which in magnitude is 44, 22, 14, 10 per cent, etc. respectively, of the centre filter. This case — "excitation curve" in the case of a truly sinusoidal input voltage resonating with a filter— is illustrated in fig. 2. The spectrogram has a character similar to that of the excitation curve of the basilary membrane of the human ear, which can be represented as consisting of a similar series of damped resonators [3]).

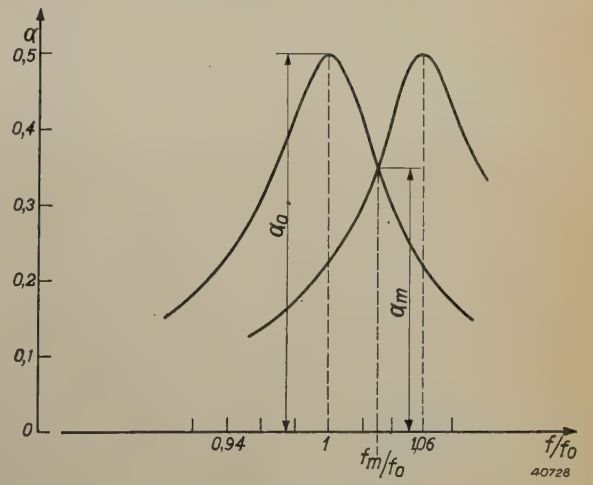

Fig. 4. With the value $q = 32$ and a distance of $^1/_{12}$ of an octave between the resonance frequencies of successive band filters, the transmission factor a_m at the point of intersection of two adjacent resonance curves is $1/\sqrt{2}$ times as large as that at resonance (a_0).

[2]) See for example R. Vermeulen, Octaves and decibels, Philips Techn. Rev. **2**, 47, 1937, graph on p. 49.

[3]) See J. F. Schouten, The perception of pitch, Philips Techn. Rev. **5**, 286, 1940, where on p. 290 such a model for the basilary membrane is discussed.

If the construction of the filters is based on a recording speed of 20 times per second, it is of course desirable that there should be no other elements in the apparatus which prevent recording at such a speed. Critical points in this respect are the outputs of the rectifiers, the input of the modulator and the electron ray tube. The rectified voltages are taken from a resistance R_2 inserted in every rectifier circuit, through which resistance the rectified current flows, while a condenser C_2 in parallel with R_2 serves to smooth the voltage to the required degree. The time constant R_2C_2 of this circuit must be so small that the condenser C_2 can be practically discharged between two recordings. R_2C_2 cannot be made indefinitely small, since R_2 must be large enough to obtain a high voltage and also in order not to affect the band filter by too high a consumption of current, and also since C_2 must be large enough to obtain the desired smoothing effect. Nevertheless, it was found possible to give the product R_2C_2 exactly the value $^1/_{20}$ sec, so that the recording of 20 pictures per second was not hindered by this. In fact, apart from the impossibility of making R_2C_2 indefinitely small, a much smaller value of R_2C_2 would not even be desirable, since then the consequences of a short-lived change in the signal disappear again so quickly that there would be a great chance that it would be unnoticed with a time interval of $^1/_{20}$ sec between successive recordings.

Similar considerations are also valid for the input of the modulator. As soon as the switch E_1 makes contact with a certain lamella of the collector, the input capacity C_3 of the modulator is loaded *via* the resistance R_3 in the connections between rectifier and collector. It was now found necessary to make C_3 large enough to limit the effects of the switching impulses occurring; at the same time, however the charging time C_3R_3 of the modulator input must be made extremely small. For the recording of 20 spectrograms per second, each consisting of about 80 measured points, only $\frac{1}{20} \cdot \frac{1}{80} = 0.0006$ sec is available for the scanning of each lamella; since there must also be sufficient space between the lamellae of the collector, the actual time of contact is only about half as long. In order to record the correct voltage value, the time C_3R_3 must therefore be chosen appreciably smaller than 0.0003 sec. With the values chosen of $R_3 = 0.22$ MΩ and $C_3 = 500$ $\mu\mu$F, R_3C_3 became 0.00011 sec, which is small enough.

Finally there is the electron ray oscillograph. For tracing one vertical line in the spectrum, with the desired recording speed of 20 pictures per second, 0.0003 sec is available according to the above. With a maximum length of the lines of for instance 4 cm the tracing speed of the oscillograph [4]) therefore amounts to 4 cm/0.0003 sec = 120 m/s. Although in ordinary cases, for instance with the electron ray oscillograph GM 3152, exposures can easily be made with such a tracing speed, in this case this is not immediately true, since we must also pay attention to the resolving power. With a length of the spectrogram of about 8 cm the width of each of the 79 vertical lines may not be greater than about $^1/_2$ mm in order that they may not overlap. With the required very fine fluorescent spot the necessary light intensity for exposures with the tracing speed mentioned could only be obtained by the use of an electron ray tube with post-acceleration [5]).

[4]) Actually, of course, the fluorescent spot moves 16 times as fast, since it makes a vibration with a frequency of 50 kc/s along the line. It comes to practically the same thing, however, for photography, whether the spot describes the line once with a given velocity or 16 times with a velocity 16 times as great.

[5]) See J. de Gier, An electron ray tube with post-acceleration, Philips Techn. Rev. **5**, 245, 1940

Relation between the length of line on the screen and the amplitude of the Fourier component

The rectified output voltage of the band filters can be modulated on the "carrier wave" of 50 kc/s in different ways. There are, however, two requirements: firstly that with a modulating voltage of $v_m = 0$ the amplitude Vd of the carrier wave should also become equal to zero; secondly that the relation between Vd and vF should have a certain character. By itself a linear relation would seem most obvious. There is, however, the objection that because of the great differences occurring in the intensity of the sound, the weak Fourier components would quickly become insignificant compared with the strong ones. If Vd increases less than proportionally with v_m, as for instance in the case of a logarithmic relation, then all intensities are dealt with equally, but there is the disadvantage that a peak in the Fourier spectrum is even more flattened than already results from the damping of the band filters (see fig. 2). An intermediate way, in which the relation between Vd and v_m begins approximately linear and then curves off towards a sort of logarithmic relation, is the most suitable.

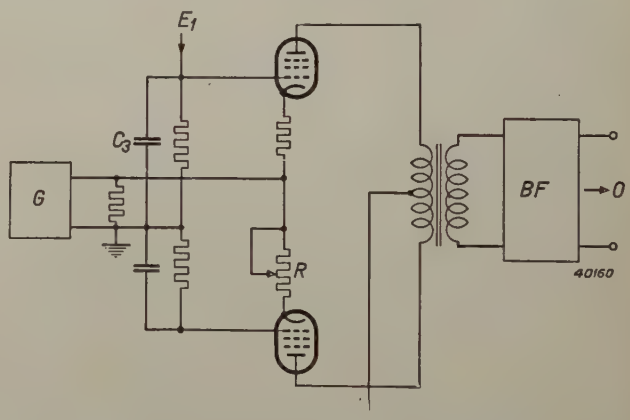

Fig. 5. Connections of the modulator. The anode alternating currents of the two valves which are excited by the carrier wave voltage of the generator G are adjusted to equal magnitude with the resistance R, so that the band filter BF receives no input voltage. By means of a D.C. voltage v_m which is fed from E_1 to the control grid of one valve, the equilibrium is disturbed and a carrier wave of a certain amplitude is therefore passed on to the oscillograph O.

Such a relation is now realized by the modulator connections shown in *fig. 5*, in which at the same time the first condition mentioned, namely that $Vd = 0$ when $v_m = 0$, is also satisfied. The voltage of 50 kc/s of the generator G is fed in the same phase to the control grids of two valves in push-pull connection working with inverse feed-back. Each valve furnishes a certain anode alternating current, but due to the compensation of the two currents

in the output transformer — which compensation can be precisely adjusted by the regulatory resistance R — no carrier wave is ordinarily transmitted to the band filter BF ($V_d = 0$). If by means of the rotating switch E_1 a D.C. voltage v_m is applied to the control grid of one of the two valves, the operating point of this is displaced on its characteristic to a point with a steeper slope, the anode alternating current of this valve becomes larger, the compensation is sufficient and the excess is transmitted as output signal (with 50 kc/s) to the band filter. If the matter is considered more carefully, in the case of the valve with inverse feed-back the relation between the anode alternating current i_a and the grid A.C. voltage v_g is given by

$$i_a = \frac{s}{1 + sR} v_g,$$

where s stands for the slope and R for the resistance in the cathode connection which effects the inverse feed-back. The slope s is chiefly determined by the grid D.C. voltage v_m and (at least in the beginning) increases proportionally with v_m. The expression $s/(1 + sR)$, however, increases less rapidly than in proportion to s and finally approaches the constant value $1/R$. From the cooperation of these two functions, upon suitable choice of the point on the characteristic at which the valve operates with $v_m = 0$, exactly the desired relation between V_d and v_m is obtained, approximately linear at first and later curving.

Actually it is not a question of the relation between V_d and v_m, but of that between the length of line on the fluorescent screen and the intensity of the corresponding Fourier component. Now the whole apparatus is about linear,

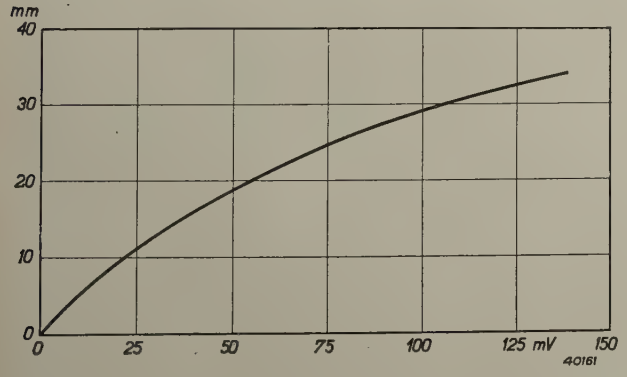

Fig. 6. Measured relation between the length of line on the fluorescent screen and the strength of a sinusoidal input A.C. voltage from the apparatus at a frequency which lies just in the centre of the transmission region of one of the band filters. The attenuator shown in fig. 1, which is inserted in front of the pre-amplifier V_1 in order to be able to regulate the input voltage of the band filters, was in this case in its extreme position (no attenuation). Furthermore, the maximum amplification of the oscillograph amplifier was operative.

thanks in part to the use of diodes (EA 50)in the rectifiers. Because of the large number of rectifiers (79) it would have seemed preferable to use blocking-layer valves, but owing to the linearity mentioned this was not done (moreover, the diode has the advantage of being less sensitive to overloading). Since the relation between the length of line on the screen and the deflecting voltage V_d on the cathode ray tube is also satisfactorily linear, the relation between the length of line and the input voltage of the whole apparatus has practically the same form as the relation between V_d and v_m. This relation as determined by measurement is reproduced in *fig. 6*.

The recording of the spectrograms

In order to make an "instantaneous exposure" of the changing sound the spectrum on the screen of the oscillograph may be photographed with a camera whose shutter must be opened for exactly one revolution of the rotating switches E_1, E_2. If it is desired to make a series of

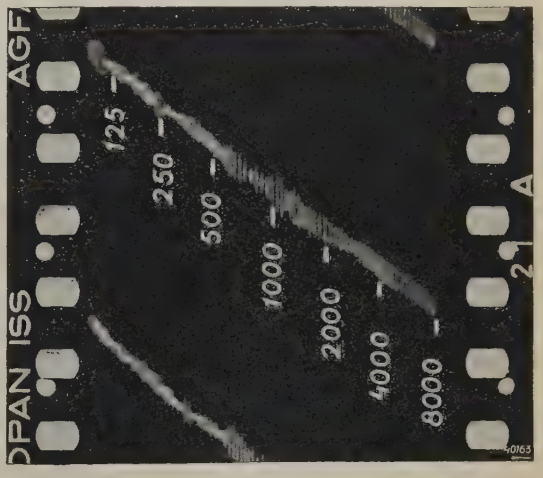

Fig. 7. Spectrogram recorded with continuously moving film. Due to the superposition of the film movement on the motion of the fluorescent spot the spectrum is recorded along an oblique line, descending towards the right. When the last spectral line has been traced the spot jumps to the left again and begins anew. The frequency scale in c/s is indicated on the film.

such exposures, and thus to "film" the sound, the film should be shifted by the height of one picture after each revolution of the switches. With the construction of the collectors here chosen, in which only as much space is allowed between the first and the last of the 79 contacts as is necessary to prevent the occurrence of short-circuiting of the source of voltage for the horizontal deflection of the spot (see fig. 1), the time available for the shift is too short, so that in each exposure the beginning of the spectrum would have to be missed or every other

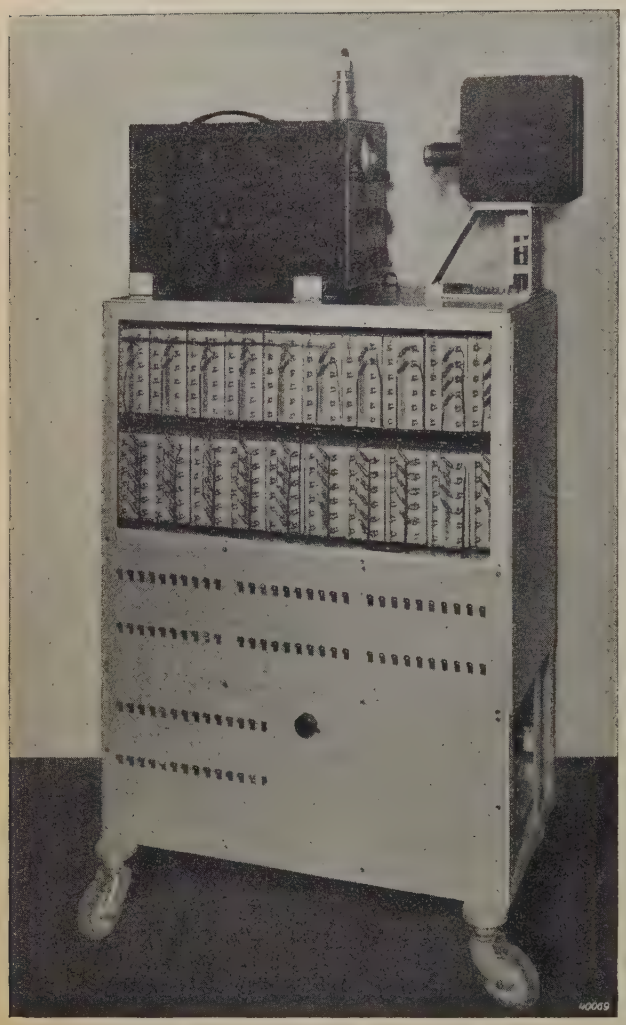

Fig. 8. In the upper part of the wheeled cabinet may be seen a large number of boxes in which the 79 band filters are housed. Underneath are the rows of switches S for listening to the filtered-out spectral parts of the sound being investigated. On top of the cabinet on the left is the electron ray oscillograph (GM 3152), on the right the film camera.

complete revolution of the switches would have to be omitted. A better and simpler solution was therefore to allow the film to move continuously in the direction of the vertical spectrum lines with permanently open camera shutter. When this is done of course a uniform movement in the direction of the film is superposed on the motion of the fluorescent spot, so that the spectra traced are pulled into an oblique position (see *fig. 7*), while, moreover, the ends of each spectral line are slightly less sharp. These features, however, constitute no disadvantage in the analysis of the diagrams.

Photographing with continuously moving film sets a sharp limit on the time of phosphorescence of the fluorescent screen. While with a discontinuously shifted film the permissible time of phosphorescence is determined by the recording time of a complete spectrogram (1/20 sec), with a continuously moving film the only permissible time of phosphorescence is that which is determined by the lack of sharpness to be tolerated at the ends of the lines, and which is therefore of the same order as the time necessary for tracing one vertical line in the spectrum (*i.e.* 1/1600 sec). In the case of the screen of the electron ray tube used by us the phosphorescence time was found to be sufficiently short.

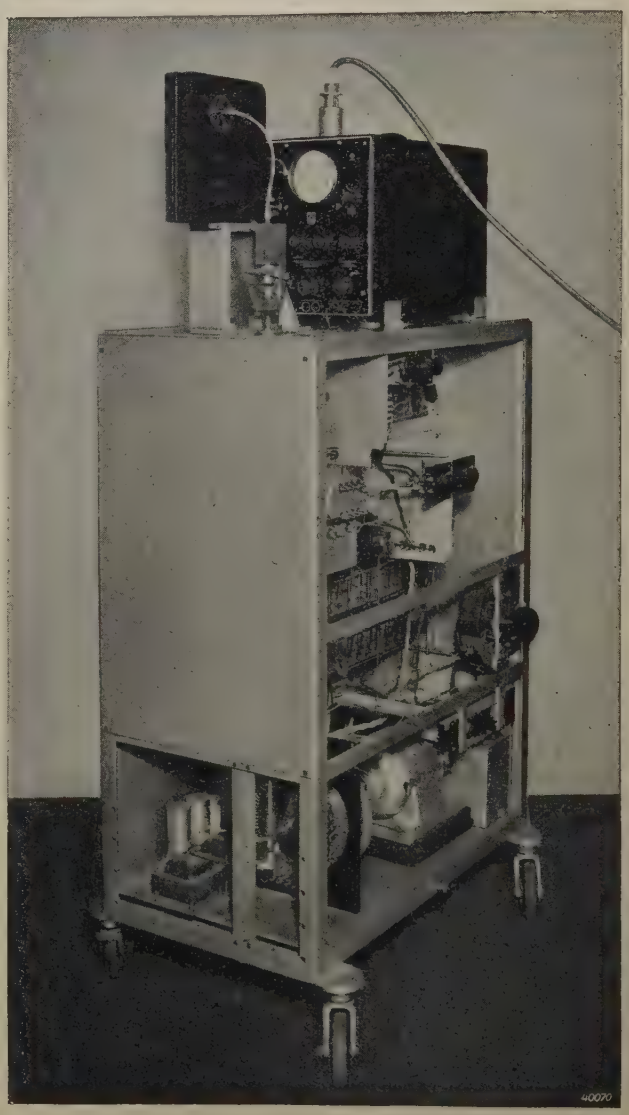

Fig. 9. On the bottom of the wheeled cabinet may be seen the motor which drives the two collectors E_1 and E_2 and, *via* a tooth-wheel transmission and a vertical axis, the film camera. In order to prevent acoustic disturbances the motor is mounted on a thick rubber plate. The collectors consist of a ring of high-frequency "Philite" in which a ring of conical copper pins is driven; with this construction wear is restricted and at the same time with little upkeep only a very low transition resistance at the contacts is obtained. In addition, on the bottom of the cabinet are the supply apparatus for the amplifiers, the modulator, the plates for horizontal deflection of the oscillograph, etc. Above are the 79 diode rectifiers. On top of the cabinet may be seen in the foreground the coupling in the driving shaft of the film camera, which may be connected and disconnected. The lead on top of the electron ray oscillograph supplies the post-acceleration voltage.

During one revolution of the rotating switches the film movement must be such that even with the largest amplitudes occurring successive spectra must not overlap. In order to ensure this once and for all at different speeds of revolution of the switches, the camera is driven, *via* a tooth-wheel transmission and a flexible shaft, by the same motor (a D.C. motor with variable speed) to the axle of which the switch arms are fastened. The camera is set in motion or stopped by means of a simple coupling mechanism.

As described in detail above, a maximum recording speed of 20 spectrograms per second can be attained. For many purposes a lower speed, for instance 10 pictures per second (thus half the speed of revolution of the switches) will suffice, and the recording speed then corresponds to the longest decay time of the filters occurring (1/9 sec with the filter for 90 c/s).

As a conclusion to this description, in *figs. 8* and *9* two photographs of the apparatus constructed are given. Several structural details are pointed out in the text below the figures.

Several results obtained with the apparatus

In *fig. 10* a number of filmed spectrograms are given which were made with the apparatus. They are the spectra of several sounds of speech, namely the vowels a, e, i, o, u, recorded at a speed of 16 spectra per second. The frequency scale is the same as that of fig. 7.

While it is generally known that the consonants are characterized for the most part only by certain introductory and transitional vibrations (most of them cannot be "held"), it is clearly apparent from the sections of film reproduced that vowels also fail to represent a completely periodic vibration. Each vowel is in fact characterized by a series of harmonic components which lie in certain formative regions, relatively independent of the pitch of the fundamental tone of the sound.

The fundamental tone, which may be quite different for male and female voices, in the case of the subject of the spectrograms in fig. 10 is about 250 c/s (peak on extreme left, band filter No. 10) for the e, i, o and u. In the case of the a during its pronunciation the fundamental tone is seen to rise slightly from 175 to 225 c/s, and in the case of oo it falls slightly from 250 to 175 c/s. Such variations in the fundamental tone are of little importance for the separate sounds of speech, but they do

[1]) The subjects of these experiments spoke the language of the Netherlands. The vowels have approximately the same sound as in French, the double o (oe in Netherlands) is the English oo as in root.

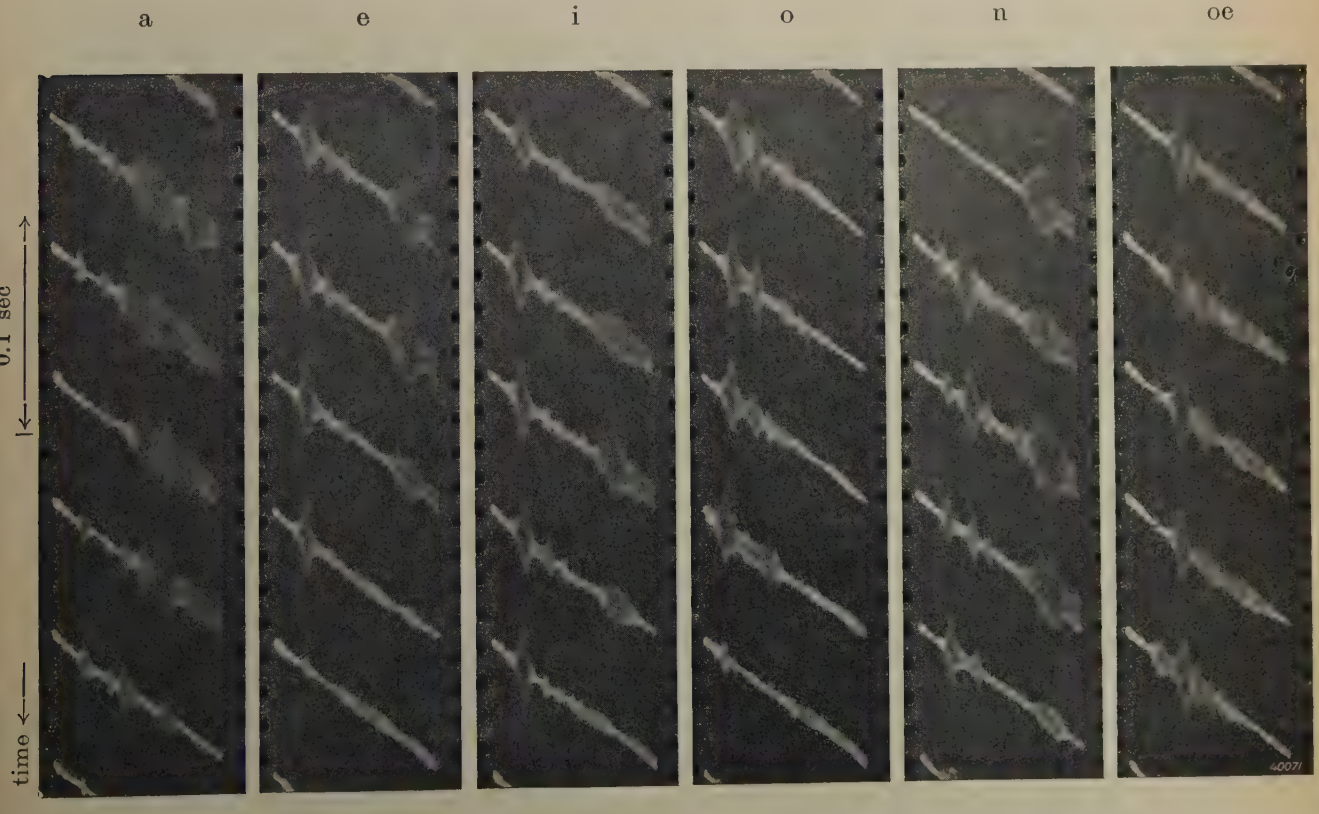

Fig. 10. Fourier spectra of several spoken vowels filmed with the apparatus. Frequency scale of each spectrum as in fig. 7. The recording speed was 16 pictures per second, so that in a vertical direction the time scale indicated on the left is valid.

play an important part in the capacity of the language for expression. This is an important point for investigation in phonetics. If the position and intensity of the other peaks in the spectrum are measured, the following data *(table I)* are found for instance for the a (third spectrum from the top) (applying the calibration curve of fig. 6).

Table I

Filter No.	Frequency c/s	Voltage mV
16	210	8
28	421	14
35	630	19.5
44	1060	75
56	2120	40
64	3360	30.5

As may be expected theoretically [6]), these frequencies are multiples of the fundamental tone (210 c/s). The strongest overtone is found at 1060 c/s, in which region lies the most important formative of the a. The weaker maxima usually occurring as well, which in this case for instance occur at 2120 and 3360 c/s, are less essential to the character of the vowel.

Upon investigation of a series of different voices we found for the most important formative of each of the vowels mentioned the frequency regions given in *table II*, column *A*. For the sake of comparison the values given by Stumpf on the basis of detailed investigations are given in column *B* [7]). It is evident that the individual differences may be quite considerable and that the frequency regions by which, according to the current conception, a vowel is characterized are anything but sharply defined. This is the more striking since in the synthetic production of vowels with the help of a number of band filters it is found that fairly accurately determined formatives are necessary for the recognition of a vowel; for example in our experiments on this subject a formative which deviated only little from 1500 c/s was necessary for the production of a clearly "pronounced" a.

Table II

Most important formative regions of six vowels, according to measurements with the apparatus described. For the main formatives our own measurements (column *A*) are to be compared with values given in the literature [1]) (column *B*),

Vowel	Subordinate formative c/s	Main formative c/s	
		A	*B*
oe	150-300	—	—
o	—	400-500	366-548
a	—	950-1498	548-1304
u	150-300	1888-2520	1843-2926
e	300-600	2378-2996	2069-2762
i	150-300	2828-3786	2192-3687

[6]) The spectra of the vowels are formed due to the fact that certain harmonics of the vocal chord vibration, which contains the fundamental tone with a large number of harmonics, are amplified by resonance of the cavity of mouth, throat and nose. See also J. de Boer and K. de Boer, The Laryngophone, Philips Techn. Rev. **5**, 6, 1940.

Such experiments with synthetic vowels also furnish a good illustration of the above-mentioned fact that the filmed spectra clearly show a fluctuation of the components during the pronunciation of a vowel. In the case of artificial vowels where this fluctuation is lacking the vowel can indeed be recognized, but the sound is not "human" in character. For the appearance of the human character the natural vibration which is given to the sound by the muscles which contract the vocal chords and determine the shape of the cavity of the mouth, throat and nose (see footnote [6]) seems to be essential [8]).

In conclusion we should like to point out that the possibilities of application of the acoustic spectrograph described here are not limited to the investigation of speech. The apparatus undoubtedly offers important possibilities for the investigation of musical instruments, of the acoustics of halls (reverberation), of interferences on connection lines or of interfering noises of machines and the like.

[7]) According to C. Stumpf. Die Sprachlaute. Experimentell-phonetische Untersuchungen, J. Springer, Berlin 1926, p. 66. His values are for vowels sung with a fundamental tone of 183 c/s. In comparing it must be taken into account that the language of Stumpf's subjects was not the Dutch but the German.

[8]) This was also confirmed in unpublished experiments by J. F. Schouten in this laboratory. Vowels were imitated with the help of the optical siren (Philips Techn. Rev. **4**, 167, 1939), in which stencils with a cut-out vibrational form were placed in a beam of light. When the stencil was fastened rigidly the sound obtained was not "human" but lifeless in character; it became much more human however, when the stencil was held in the light beam with the hand. The "vibrato" of the hand is then a substitute for the vibrato of the vocal chords and of the resonating cavities.

THE TESTING OF POWER CABLES WITH DIRECT CURRENT VOLTAGE

by W. HONDIUS BOLDINGH. 621.319.52:621.317.33:521.315.2

The requirements are discussed which must be satisfied by an apparatus for testing power cables with high voltage. A testing apparatus for 20 kV is described.

Cable testing

Newly laid high-tension cables are generally tested by applying to them for some time a D.C. voltage which is much higher than the A.C. voltage normally used on the cable. Moreover, if during use there is any indication that a defect in the insulation is beginning to make itself felt, a high D.C. voltage is also used; in this case with the purpose of burning through the insulation at the defect, so that it can be more easily localized.

The fact that D.C. voltage can be used for testing, but not A.C. voltage, is connected with the capacity of the mains being investigated. If A.C. voltage were used the capacity, which in the case of underground cables may amount to 0.2 μF per km for instance, would be charged to this high voltage twice per period. A very high wattless power would be necessary for this, which can scarcely be compensated by means of choking coils, as is ordinarily done in testing short lengths of cable during manufacture. If for example it is desired to test a high-tension cable 10 km long with an A.C. voltage of 50 c/s and 30 kV—, 250 kVA would have to be provided ; with 20 km and 40 kV— this would even be 2000 kVA. These are values of quite a different order of magnitude than the power which is necessary and sufficient to burn through a flaw (namely only about 1 kW) and for which it is still possible to construct an easily transportable cable-testing apparatus. The last mentioned power, moreover, is more than sufficient to charge a high-tension cable in several seconds to the high D.C. voltage required for the testing.

Until now for the purpose just mentioned more or less improvised apparatus was often used which was put together by the various electrical services for their own use. Since in other respects safety devices, method of operation and reliability in high power technology have been perfected to the utmost in the course of years, at first glance it may seem surprising that this has by no means been the case with cable-testing apparatus. This can be explained by the fact that the apparatus in question is used exclusively by very expert personnel, with experience in electro-technology, who easily adapt themselves to the danger of high voltage and switching complications, so that the demand for greater safety and technical convenience has remained in the background.

In recent years, however, in addition to the incidental cable examination upon the appearance of disturbances, it has become more and more customary to carry out a periodical inspection of all the cables of the high-voltage mains in order to detect insulation flaws before they lead to disturbances in the mains. As a matter of fact such routine work makes much higher demands on the safety, compactness and simplicity of the apparatus. While in the case of newly laid cables, to which according to the usual requirements the test voltage must be applied for one hour per conductor, easy operation of the testing apparatus is of practically no importance for the total working time, transportability and ease of manipulation become much more important in a periodical control of the cable network where each conductor can only be tested for a few minutes.

Requirements made of a cable-testing apparatus

We shall now examine in more detail the requirements which should be satisfied by a modern apparatus for testing high-tension cables.

1) The D.C. voltage on the cable must be able to be read off immediately under all circumstances.
2) The charging and discharging of the cable must be able to take place safely and without loose pieces of apparatus under high voltage.
3) It must be possible to protect the cable against voltages higher than necessary and desirable for the investigation.
4) It must be possible to connect the apparatus at the place where the examination is held, even with cable terminal connections which are not easily accessible, without complications caused by unprotected connection lines; up to within several metres around the apparatus any contact with high voltage must be impossible.
5) The apparatus should form a unit which requires no putting together before it can be used ,and which is as easy as possible to operate.
6) It must preferably be of such weight and dimensions that it can without difficulty be

transported in an ordinary motor-car to any point of the cable network.

With the present position of technology it is possible to construct an apparatus for voltages up to about 50 kV and a power of about 1 kW which satisfies these requirements.

In this article we shall confine ourselves to the description of a 20 kV apparatus, which is now being manufactured in series.

Apparatus for the testing of cables with 20 kV D.C. voltage

Although 20 kV is relatively low for tests as prescribed for newly laid cables (for instance according to VDE 0255), this value is, however, often used for periodical control. In this case only very little overvoltage is desired, in order not repeatedly to overload the cable heavily, which might cause it to exhibit defects prematurely. For "10 kV" multiphase-current cables which normally carry 10 kVeff between two phases, *i.e.* 5.9 kVeff and 0.3 kV peak voltage with respect to earth, a D.C. voltage of 20 kV is found to be more than enough to detect flaws in time with regular control.

The different types of connections which are used in practice for the high-voltage circuit of a cable-testing apparatus are mainly determined by the type of rectifier valve used.

If, for example, one has a valve which can withstand a voltage more than twice as high as the maximum charging voltage of the cable, one valve is needed, as indicated in *fig. 1*. A high-voltage generator for cable inspection then consists in principle of a connection in series of one rectifier valve V and a high-voltage transformer T, which in this case is loaded asymmetrically. A cable-testing installation as a rule further contains as components carrying high voltage a spark gap for measuring voltages, an earthing switch with water resistance and if necessary damping resistances.

If a larger current is to be used than the available rectifier valve can normally carry, double-phase rectification with two valves V must be used, for example according to the centre-tapped connections (*fig. 2a*). If smaller valves are preferred which can tolerate little more than the normal cable voltage, two

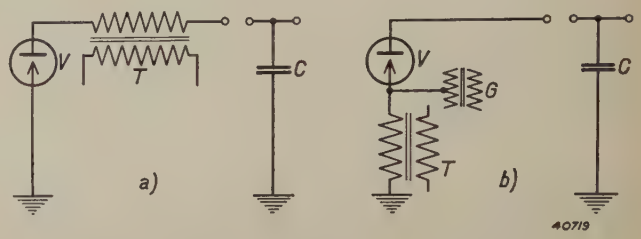

Fig. 1. Simplest connections for the excitation of a high D.C. voltage. Single-phase rectification with one rectifier valve V whose permissible counter-voltage is greater than twice the D.C. voltage to be furnished. The high-voltage transformer T is asymmetrically loaded.
a) The cathode of the valve V is earthed and two terminals of the high-voltage transformer are insulated.
b) The rectifier valve V is insulated at two terminals, while the cathode is fed by a heating current transformer G insulated for high voltage. The high-voltage transformer T is now earthed at one terminal.
C represents the capacity of the cable to be tested.

such valves V should be connected in series, and the Greinacher connection is usually employed (*fig. 2b*).

In the case of the last two connections mentioned a high-voltage transformer T with two high-voltage terminals is required. In the apparatus to be described here we have used a connection less common for cable testing in which a transformer with one high-

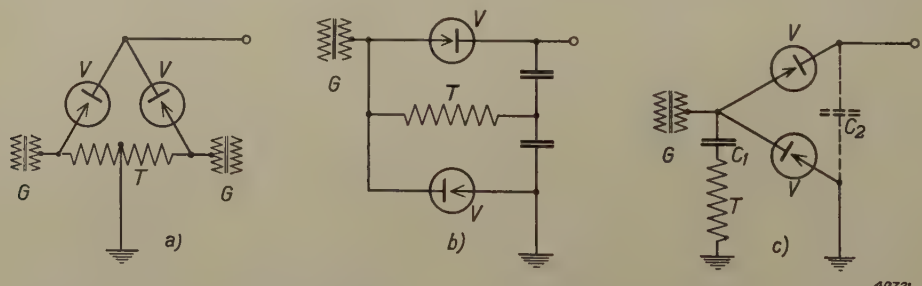

Fig. 2. High-voltage connections with two rectifier valves V.
a) Centre-tapped connections. Current doubled; high-voltage transformer T with doubled voltage, two terminals insultated and symmetrically loaded; the rectifier valves V receive the doubled counter-voltage and are fed from two heating-current transformers G.
b) Greinacher connections. The valves V receive the single voltage; high-voltage transformer T is now insulated at two terminals, has half the voltage and is symmetrically loaded.
c) Cascade connections. The rectifier valves V have the single voltage; high-voltage transformer T is here earthed at one terminal and is nevertheless symmetrically loaded.
C_1 is the cascade condenser and C_2 the smoothing condenser.

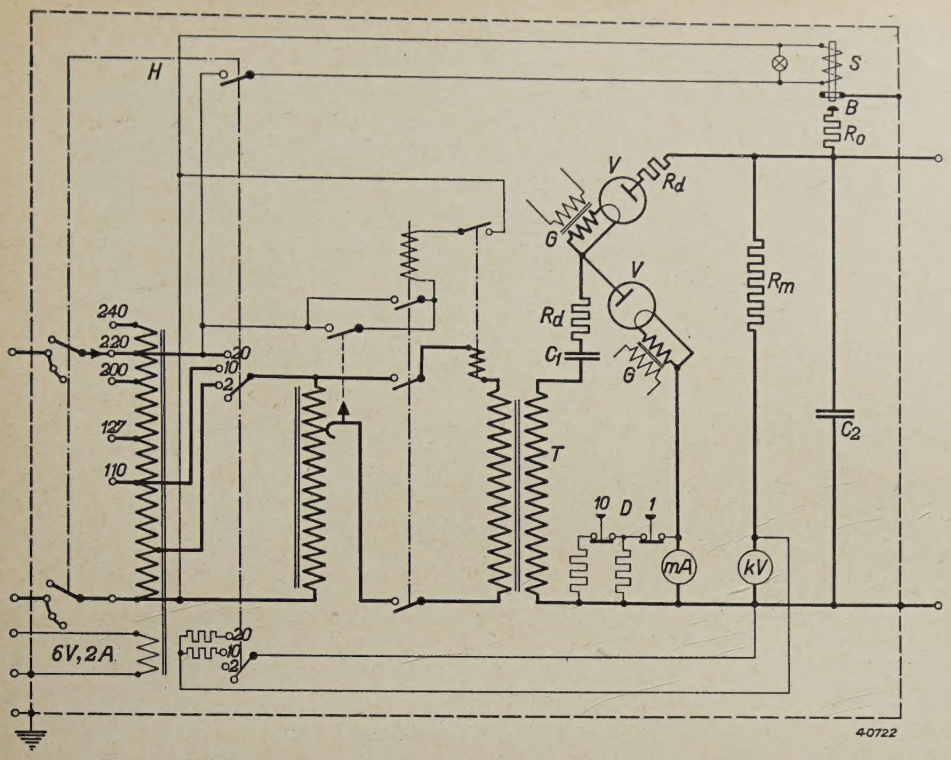

Fig. 3. Simplified diagram of the connections of the apparatus for testing high-tension cables with 20 kV D.C. voltage. V rectifier valves, T high-voltage transformer, G heating-current transformers, R_m resistance in series with the kilovoltmeter kV, mA milliammeter, H main switch, D push buttons for commutation between the measuring ranges, R_0 discharging resistance, R_d damping resistance, B adjustable voltage limiter, S magnetic switch with contact pin, C_1 cascade condenser and C_2 smoothing condenser added to permit the testing of objects with little capacity.

voltage terminal can be used. This is the so-called cascade connection (fig. 2*c*), which is also used for generating much higher D.C. voltages, as already described in this periodical [1]). These connections make it possible to use for a 20 kV generator two rectifier valves V with a maximum counter-voltage of 28 kV and a transformer T insulated at only one terminal and nevertheless symmetrically loaded.

In *fig. 3* a more complete diagram of these connections is given, while in *fig. 4* the complete apparatus is shown.

On the basis of the diagram we shall now discuss in more detail how the requirements given in the foregoing are satisfied by this apparatus.

Measurement of voltage, current and insulation resistance

The voltage is measured with the help of the kilovoltmeter kV indicated in fig. 3, which is provided with a series resistance R_m and placed on the top of the apparatus. It is thus possible under any circumstances during the testing to read off directly the actual voltage on the cable on an earthed instrument. This method of measurement is far preferable to the measurement with a spark gap or the measurement of the primary transformer voltage. Since the primary voltage regulation of the transformer T possesses three regions of regulation (2, 10 and 20 kV) the kV-meter is constructed for three corresponding measuring ranges which are automatically chosen with the selector (H) of the voltage steps. H is at the same time the main switch (*cf.* fig. 3).

Because of the direct reading of the voltage (kV) it is possible, in combination with a sensitive ammeter (mA), to determine the insulation resistance. While the mA-meter does in fact possess a measuring range up to 100 mA (upon exceeding this limit the current is automatically

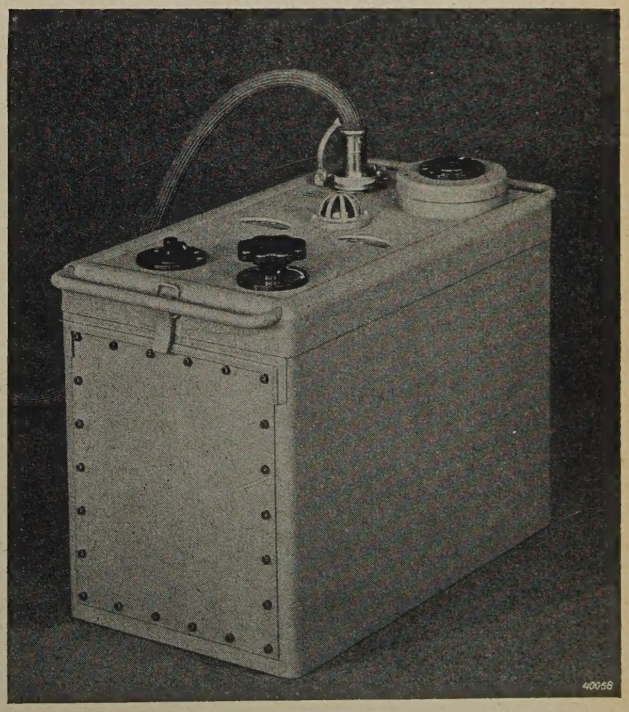

Fig. 4. The apparatus, type No. 11680, for testing high-tension cables with D.C. voltages up to 20 kV.

[1]) Philips techn. Rev. **1**, 6, 1936.

switched off), the measuring range can be reduced to 01 or 1 mA with the help of two push buttons D. In the latter case (1 mA) 20 μA per scale division is still read off, so that with negligible corona losses an insulation resistance of 100 megohms can still be observed. In order that such measurements of the insulation resistance with this apparatus need not be limited to high-tension cables with large capacity, but may in general also be carried out on insulation materials for high voltage but without appreciable capacity, a smoothing condenser C_2 is added which also guarantees a constant D.C. voltage when a current of several mA flows during the measurement.

With the measuring range up to 1 mA a combination of resistance and capacity prevents the occurence of disturbing fluctuations of the indication of the mA-meter due to fluctuations in the mains voltage. At the same time these connections form an efficient protection against damage to the meter by sudden current surges which may occur upon unexpected breakdown of a cable flaw during a measurement on the sensitive measuring range.

The two sensitive measuring instruments mentioned, here which have about 100 μA as the smallest measuring range, are made mechanically strong to resist rough usage. In order to make it possible to read them easily in the dark they are provided with an illuminated scale.

Damping and discharging resistances

In order to avoid large current impulses a water resistance is often used both for the charging and the discharging of cables, Such a more or less provisional component is in fact unsuitable for power technology. It is breakable, it cannot be used in all positions, it is difficult to fasten firmly and it may unexpectedly assume a low value due to contamination. The advantage of a water resistance is that in spite of its high resistance it possesses a large heat capacity, while that of a wire resistance, when the length of the wire is kept within reasonable bounds, becomes steadily smaller with increasing value of the resistance. For this reason a wire resistance is unsuitable for charging a spark gap, where at the moment of breakdown strong current impulses occur which would cause an intolerable heating of the wire. In the cable-testing apparatus, however, the spark gap is replaced by the series resistance R_m already mentioned, so that this advantage of the water resistance would not be decisive.

Just as for charging, so for discharging the water resistance is not necessary. For this purpose a resistance can just as well be made of wound wire with reasonable dimensions and sufficient heat capacity, especially if it need not have too high a resistance. The latter is indeed the case: if the self-induction may be neglected the size of the discharging resistance could theoretically be lowered to the wave resistance of the cable, *i.e.* to about 50 ohms, without fear of oscillations and reflections upon discharging. It is, however, unnecessary to use such low resistances ; a wire resistance of several thousand ohms with reasonable dimensions already has a heat capacity large enough to take up the heat developed upon discharge of a long cable at full voltage.

This may easily be seen on the basis of a simple calculation.

Let the specific resistance equal r ohm cm.
the cross section of the wire be q cm^2,
the length of the wire l cm,
the specific weight s g/cm^2 and
the specific heat c cal/g.

Then the resistance becomes: $R = \frac{lr}{q}$ ohm.

the weight of the wire: $G = lq\ s$ gram and
the heat capacity: $W = l\ q\ c\ s$ cal per degree.

If we now assume that the cable is so quickly discharged that the resistance first takes up all the electrical energy $E = {}^1/_2\ CV^2$ before it has time to give off a part of it by convection, the material of the resistance undergoes a short-lived temperature increase T which is given by $WT = 0.24\ E$. We can now express the cross section q and the length l of the wire in terms of the other quantities introduced above, and we find that

$$q^2 = \frac{0{,}24r}{sc}\,\frac{E}{TR}\ \text{cm}^4 \text{ en}$$

$$l^2 = \frac{0{,}24}{rsc}\,\frac{ER}{T}\ \text{cm}^2.$$

For the different resistance materials in practical use the value of s and c varies only very slightly, so that in general wire with the highest possible specific resistance r is the best. If for example we use chrome-nickel wire $r = 10\text{-}4$, $s = 8.37$ and $c = 0.1$, we find for the diameter

$$0.83\sqrt[4]{\frac{E}{TR}}\ \text{mm and for the length } 0.535\sqrt[4]{\frac{ER}{T}}\ \text{m.}$$

The net surface wound, that is without the insulation space between the windings, thus becomes

$$O = 4.45\sqrt[4]{R\frac{E^2}{T^3}}\ \text{cm}^2.$$

With a given heat capacity, therefore, the lowest resistance occupies the smallest surface. This is also clear without calculations, since with thick wire more material can be wound on a given surface than with thin wire. If for instance we have a resistance in which an energy E of 4000 joules (4 kW sec) must be taken up upon discharging a cable for 20 kV with a capacity of 20 μF where an increase in temperature of 200 °C is permissible [2]), we obtain a thickness of the wire $d = \frac{1{\cdot}76}{\sqrt[4]{R}}$ mm and a net surface wound

$$O = 42\sqrt[4]{R}\ \text{cm}^2.$$

[2]) With such a temperature increase the linear expansion is 0.3%, which is permissible without danger of the windings working loose.

For a resistance $R = 6000$ ohms, d then becomes 0.2 mm and $O = 370$ cm², while for $R = 96\,000$ ohms the wire must be half as thick and the surface wound wice as large.

The dimensions of such a resistance, which can be made practically free of induction, are small enough to allow it to be housed in the high-voltage generator (R_0 in fig. 3), so that difficulties with external assembly are avoided.

The earthing of the cable over this resistance R_0 on the earth side is by means of an electrically operated magnetic switch with contact-pin, indicated in fig. 3 by S. This switch uses zero-load current, so that the cable is automatically earthed as soon as the apparatus is switched off, while upon switching on the high voltage this earth connection is automatically broken.

Voltage limiter

The voltage limiter B in series with the discharging resistance R_0 is connected in parallel

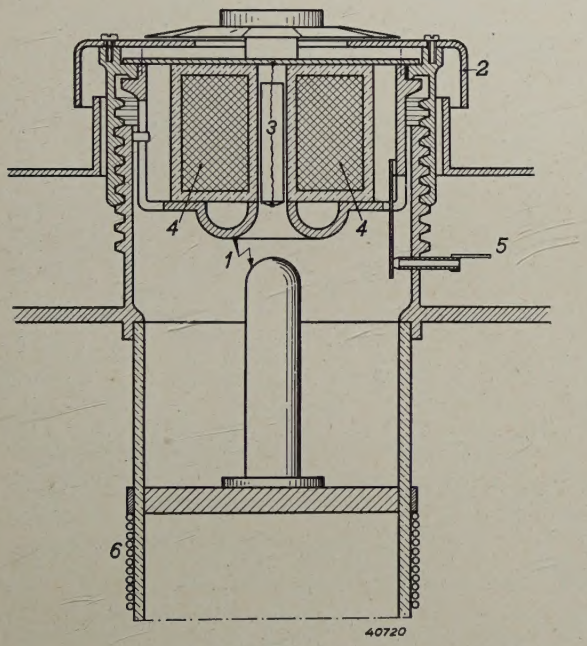

Fig. 5. Magnetic switch with contact pin. *1* Voltage limiter, *2* rotating cap for adjustment of the limiting voltage (calibrated in kV), *3* earthed contact pin, *4* solenoid for contact pin, *5* current supply for solenoid, *6* discharging resistance.

with the voltage to be measured (*cf.* fig. 3). It consists of a spark gap adjustable by hand which is calibrated in kV and by means of which too high a voltage on the cable can be avoided. The contact pin just mentioned is mounted concentrically in this spark as shown in *fig. 5*.

High-voltage protection

Since all the components of the high-voltage circuit are housed in the generator case, a single connection is sufficient to connect the generator to the cable to be tested. This connection is by means of a flexible rubber cable provided with a braided metal covering, one end of which is connected to the generator case to be earthed, and the other end to the lead covering of the cable to be tested. With sufficient length of connecting cable, therefore, the safety of anyone using the apparatus is fully ensured.

Operation

Fig. 6, which is a view of the top of the apparatus, shows that its operation has been kept as simple as possible. On the front left-hand corner is the main switch, which at the same time operates the contact pin and selects one of the three regulation regions for the voltage (2, 10 and 20 kV), while at the same time the kilovoltmeter is correspondingly adjusted (*cf.* diagram of fig. 3). In the front right-hand corner may be seen the voltage regulation knob with which the high-voltage can be increased continuously from 0 to 2, 10 and 20 kV, respectively. On the right hand in the middle is the voltmeter from which the voltage may be read off directly, while on the left of the voltmeter is the milliammeter with two push buttons for the switching

Fig. 6. View of the top of the 20 kV apparatus.

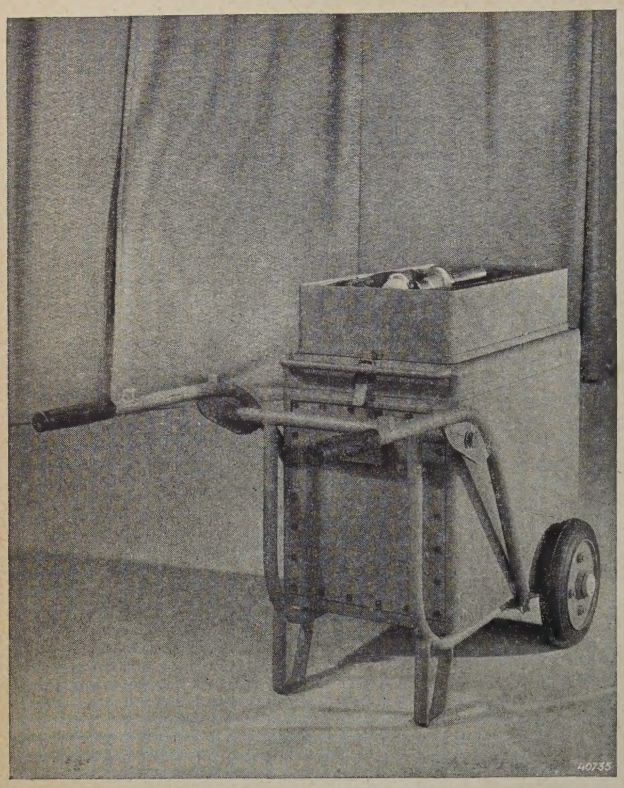

Fig. 7. The cable-testing apparatus ready for transportation.

between the measuring ranges. The voltage limiter is placed at the back and next to it the socket for plugging in the connection cable. The red signal lamp in the middle lights up when the contact pin is drawn up, so that it can immediately be seen that the cable is or will immediately be under high voltage.

Transportability

From the foregoing it is clear that the apparatus forms a closed unit which can on the one hand be connected with the low voltage mains and on the other, without further difficulties of assembly, with the cable to be tested. For easy transportation the whole can be placed on a car, which the connecting cable in a tray serving as cover *(fig. 7)*. The dimensions of the apparatus without the tray are 72 by 36 by 54 cm ; the total weight is 125 kg.

Characteristics.

In conclusion *fig 8* gives the behaviour of several electrical quantities as functions of the loading current. It may be seen that the voltage loss is relatively small, namely 0.12 kV/mA, so that there is no question of any large drop in the voltage with high currents ; this promotes the rapidity with which a flaw can be burned through. As may be seen in fig. 8, with a load of 50 mA for example the apparatus can still furnish a voltage of 16 kV, *i.e.* it can give off an energy of 800 W to a cable flaw with a resistance of 0.32 meghom, which will therefore be very quickly burned through to a lower value. Thanks to the directly readable kV-meter, it is in fact possible to follow the whole process of burning through much better than is usually the case in such investigations.

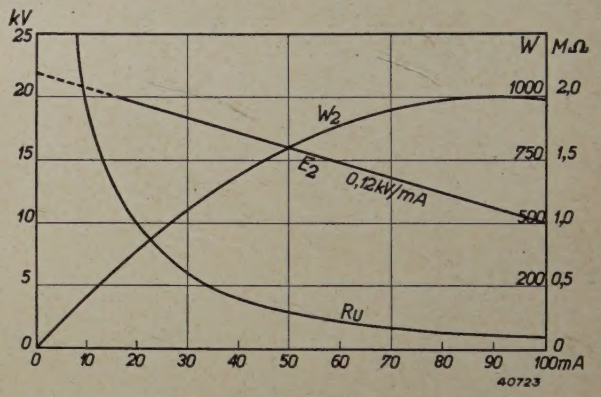

Fig. 8. The relation between various electrical quantities with the loading current, with a cable capacity of 20μF and at the highest position of the voltage adjustment. This adjustment is such that at a mains voltage 10 percent too low 20 kV zero-load can still be obtained, so that at normal mains voltage the highest zero-load voltage would be 22 kV. E_2 D.C. voltage on the cable, R_u resistance of the insulation flaw and W_2 energy for burning through the flaw. A load of 50 mA is permissible for one hour. At 18 kV the apparatus can furnish a current of 30 mA continuously.